

Precise Orbit Determination for the GEOSAT Follow-On Spacecraftⁱ

N.P. Zelensky (2), D.D. Rowlands(1), F.G. Lemoine(1), D.S. Chinn(2), S.B. Luthcke(1), G.C. Marr(3)

- (1) Space Geodesy Branch Code 926, NASA GSFC
- (2) Raytheon ITSS Corp., Lanham, MD,
- (3) Flight Dynamics Analysis Branch, Code 572, NASA GSFC

Presented by Mark Torrence (2) to 12th International Workshop on Laser Ranging (ILRS), Nov. 2000

ABSTRACT

The primary mission objective of the US Navy's GEOSAT Follow-On spacecraft (GFO), launched February 10, 1998, is to map the oceans using radar altimetry. Altimeter crossover analysis suggests GFO is capable of TOPEX/POSEIDON (T/P) class altimetry, with orbit error the largest contributor to the GFO altimeter error budget. The spacecraft tracking complement consists of on board GPS receivers, a laser retro reflector, and Doppler beacon. Since the GPS receivers have returned only limited data, satellite laser ranging (SLR), especially in combination with altimeter crossover data, provide the only means of determining high-quality precise orbits. SLR has tracked the spacecraft since April 22, 1998 with an average of 8 passes per day. Since the predicted radial orbit error due to gravity is only 2 to 3 cm, the largest contributor to the high SLR residuals (8 to 10 cm) is the mis-modeling of the non-conservative forces. SLR and other residuals also show a clear correlation with the beta-prime (solar elevation) angle. GEODYN, used for the precise orbit determination, incorporates a 3-D model of the spacecraft (macro-model), as well as an attitude algorithm describing its orientation, to better represent the non-conservative forces acting on the spacecraft. The macro-model optical properties can be adjusted (tuned) with sufficient tracking data extending over a beta-prime cycle. SLR data has been critical for tuning the spacecraft SLR antenna offset, macro-model and gravity field. The ability to use altimeter crossover data and the improved models has reduced radial orbit error from 10-15 cm to well under 8 cm. In addition, use of T/P-GFO altimeter crossover data promise even further orbit improvements. We report on the analysis of the GFO tracking data (SLR, Doppler, altimeter crossover), and on the tuning of the macro-model and gravity model using these data, with special focus on the SLR contribution.

INTRODUCTION

The launch of the GEOSAT Follow-On (GFO) satellite February 10, 1998 marks the beginning of the Navy program to develop an operational series of low-cost altimeter satellites for maintaining continuous ocean observation via the GEOSAT exact repeat orbit (Table 1). GFO provides real-time measurements of the relative ocean heights for tactical applications and absolute heights post-processed for large-scale ocean modeling. Its inclination and ground-track repeat period serve to complement altimeter datasets collected by other missions such as TOPEX, ERS1 and ERS2.

GFO carries a single frequency (13.5 GHz) radar altimeter, a dual frequency water vapor radiometer, a dual frequency Doppler beacon for operational tracking, a laser retro reflector array (LRA) and four Global Positioning System (GPS) dual-frequency receivers for precision orbit determination (POD).

The measured quantity of interest, the ocean surface above the reference ellipsoid, is in fact a combination of two measurements: the ocean surface with respect to the satellite as observed by the altimeter, and the satellite height above the reference ellipsoid determined from the satellite tracking. GFO's capability to produce precise observations of the ocean surface thus depends critically on the accuracy of the orbits produced from the Doppler, SLR, or GPS tracking. GFO pre-launch analysis anticipates an accurate altimeter product (Table 2).

Since the GPS receivers had delivered only limited data¹, SLR tracking has provided the only means for computing highly accurate orbits, and has been designated as the primary tracking system for GFO POD. The 5-cm radial orbit error estimate for SLR tracking shown in Table 2 was derived in a pre-launch simulation study² It is the Root Mean Square (RMS) error over one day.

The Space Geodesy Branch at Goddard Space Flight Center (GSFC) has been given the task of improving GFO POD. This work

ⁱ The authors acknowledge Yoaz Bar-Sever of the Jet Propulsion Laboratory and Scott Mitchell of Ball Aerospace for information pertaining to modeling of the GFO attitude. J. Andrew Marshall (now at Lockheed-Martin, Denver) developed the preliminary (untuned) macro-model for GFO.

has included pre-flight orbit error analysis, tuning a "macro-model" of the approximate spacecraft geometry and surface properties in order to better model the nonconservative forces, tuning the gravity model, computing the SLR based Medium Precision Ephemeris (MOE) on a daily basis for use on the NAVY NGDR and NOAA IGDR altimeter products, and providing the SLR based precise ephemeris (POE) for the CalVal evaluation efforts.

This paper reviews the analysis of GFO tracking data (SLR, Doppler, altimeter crossover) and tuning of the various models, with special emphasis on the SLR contribution. Without SLR tracking, a precise GFO altimeter product would not be possible.

ORBIT MODELING AND ANTICIPATED ERRORS

Orbit accuracy depends on quality of the tracking and fidelity of force/measurement modeling. GEODYN³, a state-of-the-art least squares orbit determination and geodetic parameter recovery program, developed and maintained at GSFC, is used for GFO POD. Table 3 shows a summary of the POD models.

Several gravity fields were tested, EGM96⁴, TEG3⁵, JGM3⁶, and PGS7609G, a GSFC combination model based on EGM96 but with additional TDRSS satellite tracking data from the EUVE, ERBS, XTE, GRO, and TRMM satellites. PGS7723c, a preliminary field, is PGS7609g tuned using GFO SLR, Doppler, and altimeter crossover data. Although covariance projections indicate that orbit error due to gravity will be only 2-5 cm (Figure 1), the error structure will be complex, and include a geographically correlated component. By spherical harmonic order, the radial orbit error due to gravity is highest at order 1, and in the vicinity of the k=2 resonance (near order 29) (Figure 1). Tuning with GFO tracking data reduces this error.

Nonconservative forces acting on GFO consist of radiative forces and atmospheric drag. Radiative forces include solar radiation pressure, the Earth's albedo (reflected light) and infrared radiation, and other secondary effects such as thermal imbalance in emission from spacecraft surfaces. Secondary effects are not modeled for GFO. The macro-model approximates GFO's surface geometry and material properties using eight plates (Figure 2). Each plate has been assigned a body-fixed orientation, area, and specular and diffuse reflectivity coefficients based on pre-launch engineering information. All plate interaction effects, such as shadowing and multiple reflections, are ignored. The total acceleration with respect to the center of mass (CoM) is computed by summing vectorially the force acting on each plate, taking into account each plate's area, angle of incidence and material properties. Throughout the orbit and over a Beta prime cycle, radiation will be incident to a changing orientation of the macro-model as computed using an analytical attitude model. Beta prime is the angle to the sun from the orbit plane (Figure 3), and for GFO shows a period of about 336 days.

As shown in Figure 4, the largest nonconservative force acting on GFO is by far due to solar radiation pressure. Since the solar radiation pressure is so large, even a small error will have a significant impact. The error for the macro-model should be 10 to 20 percent of the radiative force. For instance, the *a priori* macro-model for TOPEX was meticulously constructed using finite element modeling and could only account for 90% of the radiative forces⁷. However, after tuning, the TOPEX macro-model is believed to account for over 95% of the radiative forces⁸. The approach taken for the *a priori* GFO macro-model construction was much simpler and without application of finite element modeling. Even a 5% mismodeling of the solar radiation pressure would constitute a considerable source of error, requiring the adjustment of sufficient empirical acceleration parameters for reducing orbit error to an acceptable level for POD⁹.

It has been shown in a previous study¹⁰ that given the 1999 level of SLR tracking, orbit error is due primarily to mis-modeling of the radiative forces acting on the satellite, followed by mis-modeling of the gravity field. The same study (Ref. 10) also shows that following adjustment of the LRA offset to spacecraft Center of Mass (CoM), any error in the SLR measurement modeling remains very small including error in the analytical attitude model. Two vectors are involved for defining the Laser Retro reflector Array (LRA) position with respect to the spacecraft CoM: 1) the location of the LRA phase center with respect to the spacecraft body-fixed coordinate system, and 2) the location of the spacecraft CoM in this coordinate system. The LRA is fixed and only the location of the CoM changes with time, based on propellant usage. We estimated the LRA phase center from SLR tracking, and this estimate would accommodate to first order changes in the CoM for which we do not have detailed information. One month (June 1998) was sufficient to determine the LRA offset, reducing the SLR fits and the residual mean over the several months shown (Figure 5). The LRA consists of nine corner cubes arranged hemispherically¹¹, and is expected to have a stationary phase center, independent of the tracking geometry.

TRACKING DATA AND POD STRATEGY

GFO POD relies on SLR tracking provided by a global network of NASA and foreign stations (Figure 6). Unfortunately the

tracking has been more sparse than anticipated showing an average of about eight passes per day. Operational tracking Doppler data from the three stations (Guam, Point Mugu California, and Prospect Harbor Maine) although noisy (2 cm/sec) is also abundant, and serves to slightly strengthen the SLR solution. After 40% of the data is edited, we typically use nine Doppler passes per day. The Doppler station positions have been adjusted to the SLR frame using three months of Doppler data and SLR-determined orbits that were held fixed in the solution.

The recent dramatic increase in SLR tracking has been very good news for GFO POD, growing from an average of 7 passes/day for 1998 and 1999 to over 9 passes /day for 2000 and 2001. The 33% increase in tracking for 2000 is accompanied by a 22% increase in the number of tracking stations (see Table 4 and Figures 6 & 7).

Given the SLR tracking density, an arc length of five days was selected over shorter arcs to increase the dynamic strength of the solutionⁱ. Arc lengths of nine and ten days would also be suitable, however the frequency of satellite events over 1998 and 1999, such as computer resets or maneuvers which are not modeled for POD, have allowed only a few uninterrupted ten day spans.

Altimeter crossover data, computed by differencing altimeter ranges from an ascending and intersecting descending pass interpolated to a common geographic point, can be used to supplement the SLR and Doppler data for POD. Continuous altimeter tracking only began in mid-December '99, up to which time had been somewhat sporadic. GFO crossovers provide dense spatial coverage and promise a high accuracy productⁱⁱ (Figure 8). Crossovers used in POD are edited in regions which have high sea surface variability (greater than 20cm) and in shallow seas (1000m or less).

The solution strategy, with the objective to minimize orbit error, was developed considering the strength of the tracking data. Several parameterization schemes were tested and the one finally selected for SLR is summarized in Table 3. According to this strategy orbit error is minimized by adjusting, in addition to the orbit state, atmospheric drag scale coefficients and empirical one cycle per revolution (1cpr) accelerations for both the along-track and cross-track components. The empirical and drag terms absorb much of the residual accelerations remaining from the mismodeling of the various forces and greatly reduce orbit error¹². With perfect tracking data, the more closely spaced in time, the better the empirical accelerations will remove orbit error. Imperfection in data and coverage limit the capability of empirical acceleration parameters to recover orbit error. Since the adjusted empirical acceleration terms capture information about the residual accelerations, they can reveal characteristics of the mismodeled forces. For the same reason they should be left out of solutions designed to tune the macro-model.

No single test can uniquely gauge orbit accuracy. This analysis uses SLR residuals, or the misclosure between the highly precise observed and computed ranges, altimeter crossover differences (Table 5), and orbit differences between arcs sharing one day of overlapping data, to indicate the level of orbit error. Overlap orbit differences identify the least amount of orbit error shared by the two arcs across the overlap period, as common errors will cancel

Gravity error does not explain the considerable variation from arc to arc in the SLR fits and radial orbit differences (Figure 9), and as shown in a previous study (Ref. 10), is due to radiative force mis-modeling. Sparse SLR tracking limits the capability for removing these residual accelerations by restricting the number of empirical accelerations, which can be adjusted in the orbit solution. Including altimeter crossover data significantly strengthens the solution and can lead to far better orbits (Figure 10), however the GFO crossover data should be used with caution. It is believed about 40%-60% of the ionosphere refraction effect is not removed from the altimeter data with the IRI95 model. This residual ionosphere day/night (descending pass / ascending pass) effect will directly contribute to a once per orbit revolution error (1/rev) when crossovers are used in the solution. Nonetheless the orbit improvement gained appears to overshadow any orbit error induced with the use of crossover data (Figure 10). Thus including crossover data allows the adjustment of more empirical parameters to better remove non-conservative force model error. It is important to note that for solutions which include and which do not include crossover data, orbit accuracy remains correlated to the number of SLR points present (Figure 11)! In the combination solution the presence of SLR data probably acts to constrain the effect of the ionosphere error contained in the GFO altimeter crossovers.

MACRO-MODEL TUNING

The macro-model represents the GFO spacecraft as an eight surface composite (Figure 2). It approximates the spacecraft

i. In cases of sparse tracking one can usually rely on the fidelity of the dynamic force models to determine a better orbit over a longer span. Over a shorter arc, the solution may be ill determined, and the orbit error very large over periods with no data.

ii GFO IGDR altimeter data obtained from John Lillibridge, NOAA.

geometry and surface material properties to better model the surface force effects due to solar and terrestrial radiation pressure, and due to atmospheric drag. Each surface (or plate) had been assigned an orientation with respect to the satellite fixed frame, an area, and a specular and diffuse reflectivity coefficient based on pre-launch engineering specifications. The material properties of each plate are assumed to be homogenous, representing an average value. In tuning, these average values are adjusted to best fit the GFO tracking data using an orbit determination (OD) solution strategy to insure the mismodeled nonconservative forces are not absorbed in empirical parameter adjustments. Therefore the macro-model is tuned to the residual satellite acceleration history which is based on orbit errors sensed from the spacecraft tracking data.

OD parameterization suitable for macro-model tuning adjusts the orbit state, and one drag coefficient (C_D). The solar radiation pressure coefficient (C_R), which should remain constant, is fixed to a value of 1.0. Upon solution convergence, GEODYN writes out the normal equations for the orbit (state, C_D) and panel (area, specular, diffuse) parameters for each arc. These normal equations were combined from arcs sampled over the Beta prime cycle and the selected panel parameters estimated using Bayesian least squares. A preliminary sensitivity study was performed using the combined normal matrix from four well-spaced arcs to help identify panel parameters that were to be estimated. Assuming a specified allowed percent change in each respective panel parameter *a priori* value, and using only the left-hand side diagonal (variance) terms of the normal matrix, the resulting "uncorrelated weighted variance" is computed in order to compare parameter sensitivity, or change in residual variance, with respect to parameter adjustments. The *a priori* surface area assigned to each plate is believed to be relatively well determined with about a 10% error. There is much greater uncertainty for the *a priori* specular and diffuse reflectivity coefficients, computed as an aggregate average of these properties for each surface. The area is allowed to change by 10% and the reflectivity coefficients by 100% for the sensitivity analysis. As shown in Figure 12, specular coefficients for four parameters representing the solar array, the bottom plate (+z facing Earth), and the top and bottom sides of the altimeter antenna reflector, are likely candidates for the macro-model tuning adjustment.

The solar array specular reflectivity coefficient was adjusted using 31 SLR+Doppler arcs, 8 of which include Crossover data, spanning over 20 months (May 22, 1998 to February 6, 2000) or well over the 336 day Beta prime period. The preliminary tuned macro-model shows improvement in SLR fits, even for solutions adjusting empirical parameters (Figure 13). Note that the *a priori* macro-model also shows improvement over the "cannonball" or spherical model, which would have been used in the absence of a macro-model (Figure 13).

Even though the tuned macro-model shows improvement in SLR fits, the recovered empirical acceleration amplitudes (Figure 14) and phases (Figure 15) are strongly correlated with Beta prime. This indicates that the solar radiation pressure still remains the largest mis-modeled force, and that further tuning may be warranted.

As the absolute value of Beta prime increases from zero to 80+ degrees the solar radiation pressure (and the mismodeled effect) will change its projection from predominately along-track and radial directions to cross-track (Figure 4). The adjusted empirical accelerations should thus decrease in magnitude in the along-track component (Figures 14 & 15), and increase in the cross-track. The associated phase (with respect to orbit angle) will remain constant from arc to arc until the spacecraft enters the full sunlight regime. The observed phase coherence (Figure 15) indicates that the force error preserves the same orientation with respect to orbit plane from arc to arc, which in fact solar radiation pressure does. As the spacecraft reaches full sunlight (near $|\pm 65^\circ|$ Beta prime), the recovered along-track acceleration magnitude becomes very small and for which the phase is not well determined. The along-track acceleration changes phase between increasing/decreasing Beta prime (Figure 15). In another study tuning the TDRSS macro-model¹³, a continuous phase was also observed in the recovered 1cpr along-track acceleration prior to tuning. After tuning, the recovered acceleration magnitudes were small and the phases showed no coherence.

GRAVITY MODEL TUNING

A preliminary gravity model, PGS7723C, was tuned using PGS7609G and GFO SLR, Doppler, and Altimeter Crossover data spanning 990616-990820, 991205-991210, and 000106-000205. Covariance projections show a significant improvement in orbit accuracy, specifically in order 1, near order 29 (Figure 1). Looking at several gravity fields, the SLR and Crossover fits show a marked improvement for the tuned field (Table 6). In addition tests using another satellite, TOPEX, also show some improvement in the SLR and altimeter crossover fits (Table 6) suggesting that PGS7723C may not only be a better tuned model for just GFO, but may represent a better gravity field.

Combining GFO with TOPEX altimeter data (Table 7) forms TOPEX-GFO altimeter crossover data. Since the TOPEX geographically correlated orbit error is believed to be less than 1 cm, it may be possible to differentiate the GFO geographically correlated error by geographically mapping the TOPEX-GFO altimeter crossover residuals. Indeed, after averaging crossover residuals from five 10-day arcs over $5^\circ \times 5^\circ$ blocks, geographic structure becomes apparent for both PGS7609G and to a lesser

degree for PGS7723C (Figure 16); the difference between the two corresponding to the difference in orbits (Figure 16). Figure 16 illustrates a significant, approximately 1.2 cm RMS reduction in geographically correlated orbit error.

ANTICIPATED IMPROVEMENTS

GFO altimeter crossover fits suggest the total (variable + geographically correlated) radial error can be between 4-5 cm with good SLR tracking (Table 5). It is possible to combine GFO with TOPEX altimeter data to form TOPEX-GFO altimeter crossover data (Table 7). From the well-defined and accurate TOPEX reference it may be possible to better calibrate the GFO altimeter corrections, to better tune the GFO macro-model and gravity field, and to better determine GFO orbits. Preliminary tests show that in the very least, the quantity of crossover data is increased 3-fold with the addition of TOPEX-GFO crossovers, further strengthening the orbit solution (Figure 17).

SUMMARY

The Space Geodesy Branch at Goddard Space Flight Center (GSFC) has been given the task of improving GFO precision orbit determination. Pre-flight orbit error analysis preceded the current work which involves tuning a "macro-model" of the approximate spacecraft geometry and surface properties in order to better represent the nonconservative forces, as well as tuning the gravity field. Since GPS receivers have delivered only very limited tracking data, SLR tracking offers the only means with which to compute precise orbits for this spacecraft. SLR data in combination with altimeter crossover data was successfully used to tune the preliminary macro-model and gravity field. The radial orbit accuracy is estimated to be 4-8 cm using the latest models and including altimeter crossover data. Use of TOPEX-GFO crossover data is anticipated to further help GFO model tuning and GFO precision orbit determination.

The large increase in SLR tracking since 1999 has been very welcome as SLR tracking density, even in combination with altimeter crossover data, determines the limit for orbit accuracy. Without SLR tracking, neither precise orbits nor a precise altimeter product would be possible for GFO.

GFO POD Points of Contact:

- **Frank Lemoine** flemoine@geodesy2.gsfc.nasa.gov
- **Nikita Zelensky** nzelensk@geodesy.gsfc.nasa.gov

ABBREVIATIONS AND ACRONYMS

Abbreviations found in this paper are normally defined after the first use of the technical term.

CoM	center of mass
ERBS	Earth Radiation Budget Satellite
EUVE	Extreme Ultra-Violet Explorer
GEOSAT	Geodesy Satellite
GFO	GEOSAT Follow-On
GPS	Global Positioning System
GRO	Compton Gamma Ray Observatory
GSFC	Goddard Space Flight Center
LRA	laser retro reflector array
NASA	National Aeronautics and Space Administration
OD	orbit determination
POD	precision orbit determination
RMS	root mean square
SA	solar array
SLR	satellite laser ranging
TDRSS	Tracking and Data Relay Satellites System
TOPEX	Ocean Topography Experiment
TRMM	Tropical Rainfall Measuring Mission
XTE	Bruno B. Rossi X-ray Timing Explore

TABLES AND FIGURES

Table 1 GEOSAT Exact Repeat Orbit

Orbit parameter	value
Altitude	800 km
Eccentricity	0.0008
Inclination	108 deg
Repeat Period	244 revs in 17 days

Table 2 GFO Pre-Launch Altimeter Error Budget ⁱⁱ

Component	Source	Error (cm)
Altimeter instrument noise	Ball	1.9
biases	Ball	3.0
sea surface (EM & skewness)	TOPEX	2.3
Media troposphere	Ball	2.0
ionosphere	Ball	1.7
SLR POD (radial orbit)	GSFC	5.0
Total RSS		7.1

Table 3 GFO Precise Orbit Determination Modeling

Model Category	Description
Geophysical models Gravity Ocean/Earth Tides Atmospheric density Spacecraft geometry and surface forces Station Coordinates Earth Orientation Parameters Planetary Ephemeris	PGS7723C (PGS7609G + GFO SLR, Altimeter Crossover, and Doppler tracking data) PGS7723C resonant + Ray '99 background terms ¹⁴ MSIS-86 ¹⁵ GFO Preliminary tuned macro-model CSR95L02 SLR solution frame ⁱ CSR95L02 from LAGEOS tracking DE403
Measurement Model SLR Doppler Altimeter Crossover	<i>A priori</i> CoM, estimated LRA offset, analytical attitude <i>A priori</i> CoM, <i>a priori</i> beacon offset, analytical attitude <i>A priori</i> CoM, analytical attitude, GEODYN Dynamic Crossover model
Tracking Data Weights SLR Doppler Altimeter Crossover	10 cm 2 cm/sec 10 cm
Estimated Parameters	Orbit state, Atmospheric drag C_D per day (or more frequently data permitting) Along-track 1cpr empirical acceleration per arc Cross-track 1cpr empirical acceleration per arc Doppler measurement and troposphere bias per pass

i. CSR95L02 is the SLR station position and velocity frame used to compute the TOPEX/POSEIDON precise orbits, Richard Eanes, CSR, 1995.

ii. An official GFO altimeter system error budget has yet to be published. The values shown here have been compiled from an internal Ball document provided by Scott Mitchell, from the T/P Mission Plan, and error simulations performed at GSFC (Ref 2).

Table 4. SLR Tracking Summary

Year	Days	Stations	Passes
1998	254	33	1829
1999	365	32	2625
2000	366	39	3485
2001	59	27	543

Table 5 GFO-GFO Altimeter Crossover Error Budget

Error Source	altimeter variable error (cm)	
	range	crossover difference
Non-orbit		
ocean + noise	3.5	5.0
ionosphere	1.7	2.4
Orbit	3.9	5.5
RSS total		7.8

Table 6. Gravity Field Tests

gravity field	radial orbit error projected from 70x70 gravity covariance (cm)	data RMS (cm) combined results over five 10-day arcs			
		TP crossover	TP/GFO crossover	GFO crossover	GFO SLR
JGM3	4.97	6.172	8.449	8.513	7.422
EGM96	2.61	6.144	7.705	8.267	6.967
PGS7609G	2.61	6.155	7.740	8.256	6.747
PGS7723C	1.92	6.128	7.224	7.803	5.884

Table 7. Altimeter Range Modeling for TOPEX-GFO Crossover Processing in GEODYN

Model	TOPEX ⁱ	GFO ⁱⁱ
Ocean tide + tidal loading	CSR 3.0 (GDR)	same (IGDR)
Earth Tide	Cartwright (GDR)	same (IGDR)
Dry troposphere	FMO (GDR)	NCEP (IGDR)
Wet troposphere	TMR (GDR)	NCEP ⁱⁱⁱ (IGDR)
Ionosphere	dual frequency (GDR)	IRI95 (IGDR)
Inverse barometer	f (dry troposphere)	same f function
EM bias	Walsh (GDR)	5% SWH
Orbit	fixed ^{iv}	adjusted
Range bias	fixed ^v	adjusted
Timing bias	fixed (GDR time tag)	adjusted

ⁱ TOPEX GDR

ⁱⁱ GFO IGDR from NOAA

ⁱⁱⁱ TMR value also available

^{iv} POE has 2-3 cm radial accuracy

^v routinely computed per cycle by PODPS based on the POE orbit

Figure 1. Gravity Orbit Error Covariance (to 70x70) Projection

Gravity Field	GFO Orbit Error (cm)		
	Radial	Cross-Track	Along-Track
JGM3	4.97	23.80	42.61
TEG3	3.48	21.42	42.76
EGM96	2.61	8.94	17.72
PGS7609G	2.61	8.93	16.44
PGS7723C	1.92	8.70	15.59

GEOSAT radial orbit error from gravity field covariances to 70x70

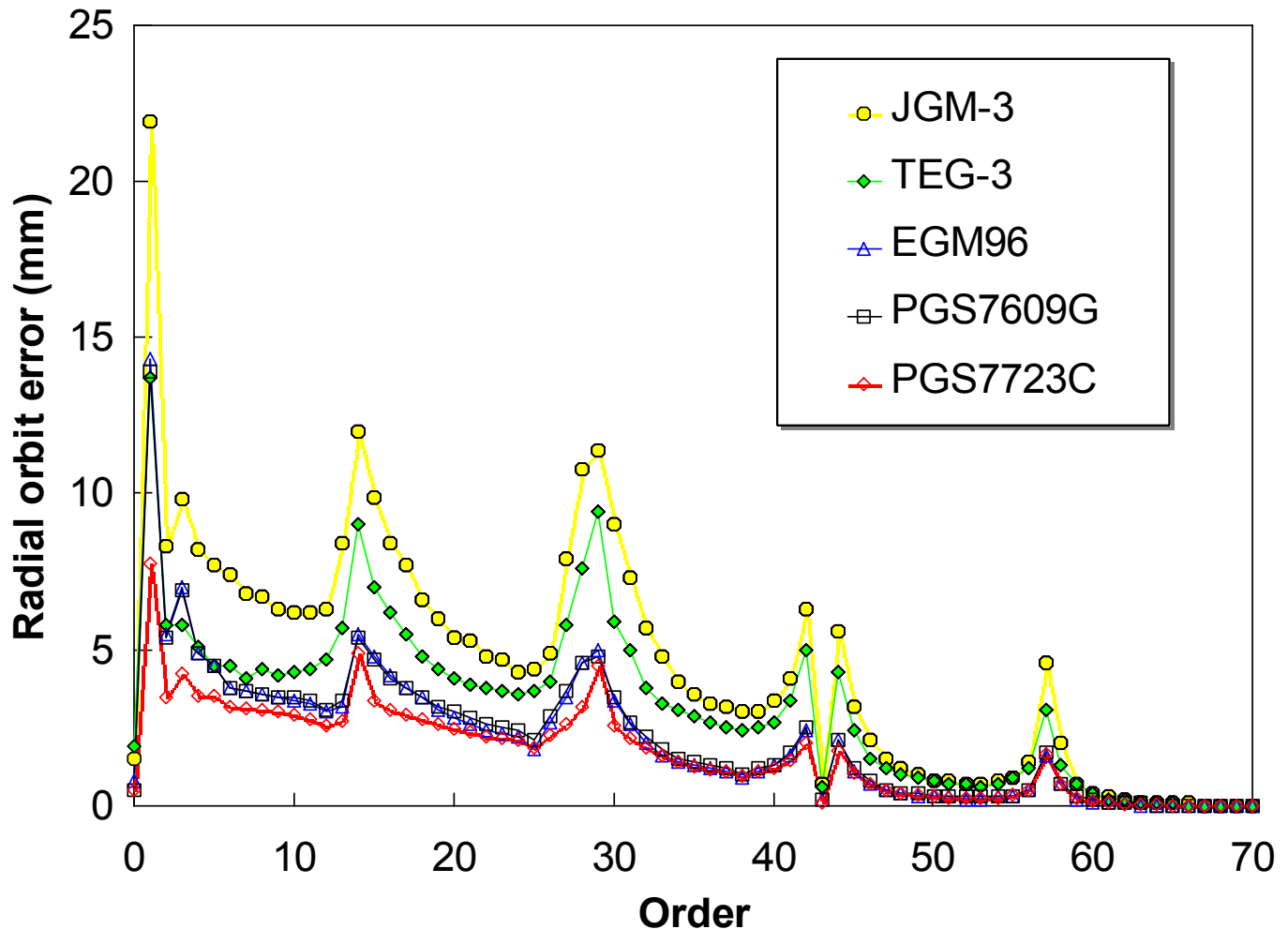
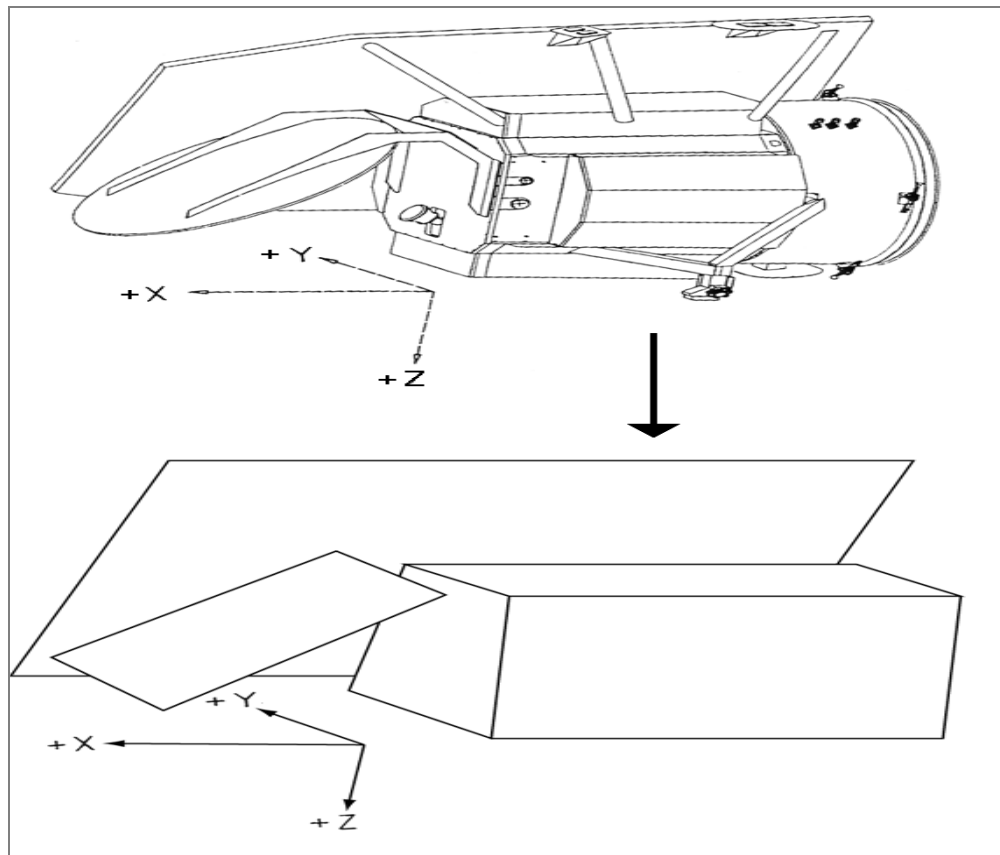


Figure 2. GFO Macro-Model Approximation



Acceleration due to radiation pressure on a flat plate:

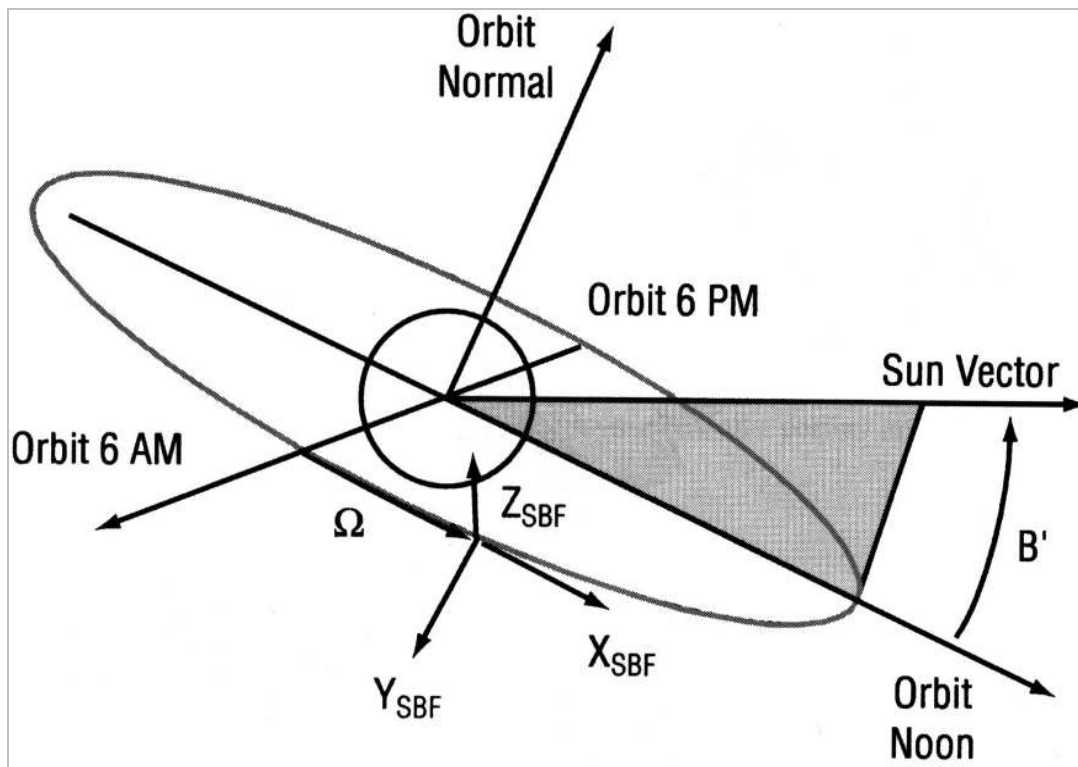
$$\Gamma = -\frac{\Phi A \cos \theta}{Mc} [2(\delta/3 + \rho \cos \theta) \mathbf{n} + (1 - \rho) \mathbf{s}]$$

where

- Γ = acceleration (m/s^2)
- Φ = radiation flux from source
- A = surface area of flat plate (m^2) *
- θ = incidence angle (surface normal to source)
- M = satellite mass (m)
- c = speed of light (m/s)
- δ = diffuse reflectivity *
- ρ = specular reflectivity *
- \mathbf{n} = surface normal unit vector
- \mathbf{s} = source incidence unit vector

* are the adjustable macro model parameters

Figure 3. Orbit geometry



GFO Beta Prime Cycle

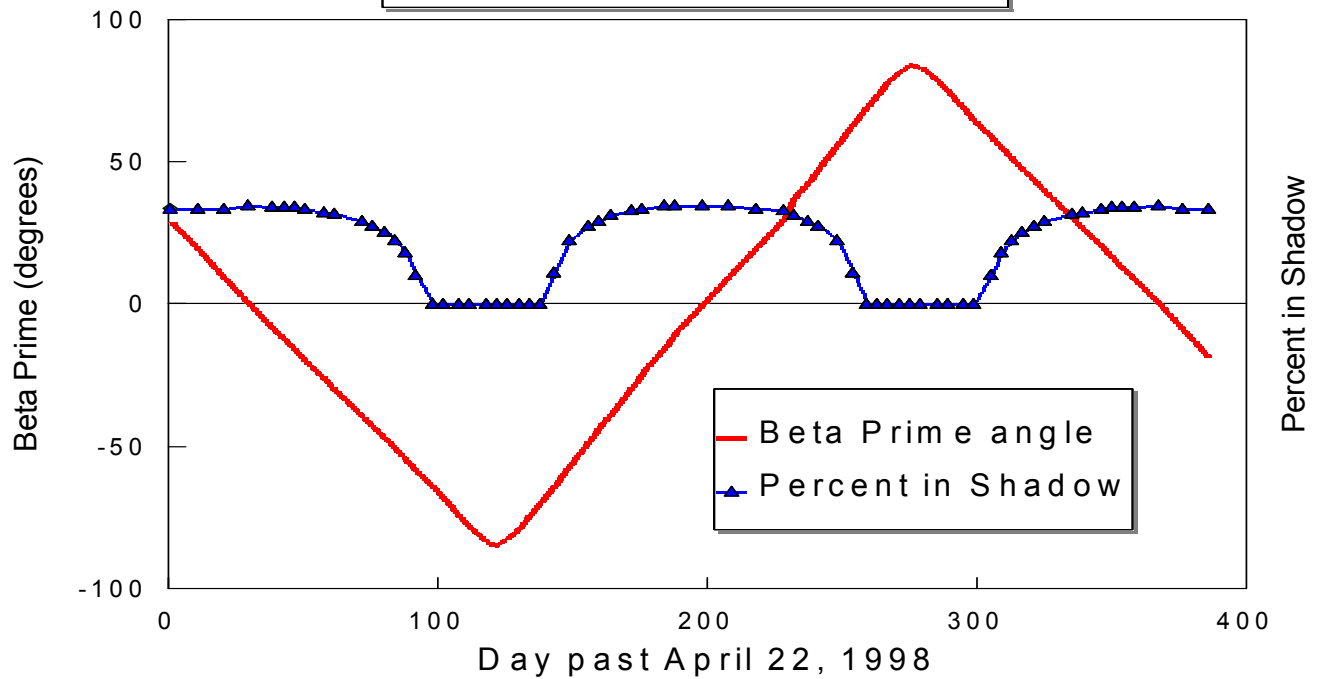
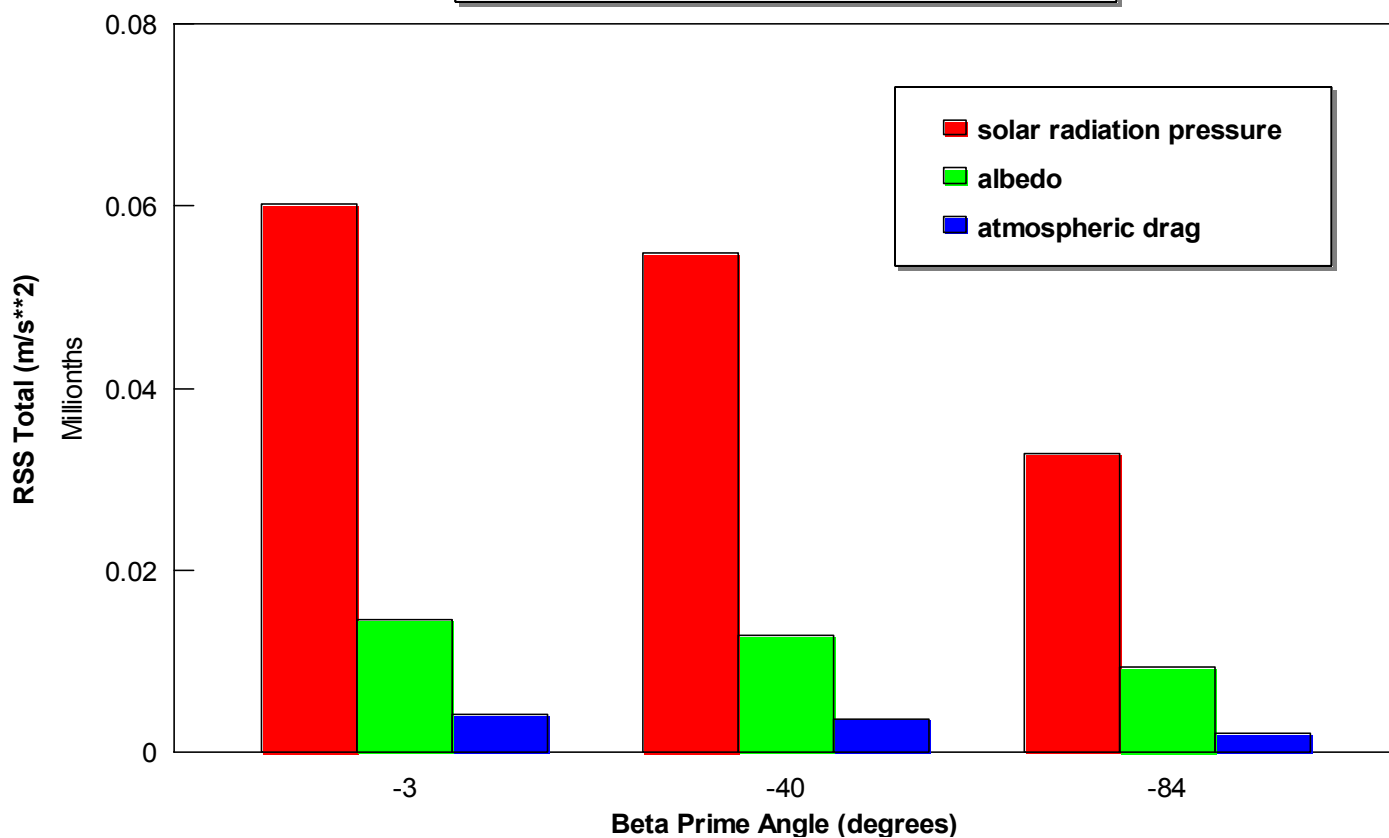


Figure 4. Non-conservative forces acting on GFO

GFO surface force accelerations



GFO Solar Radiation Pressure Along-Track

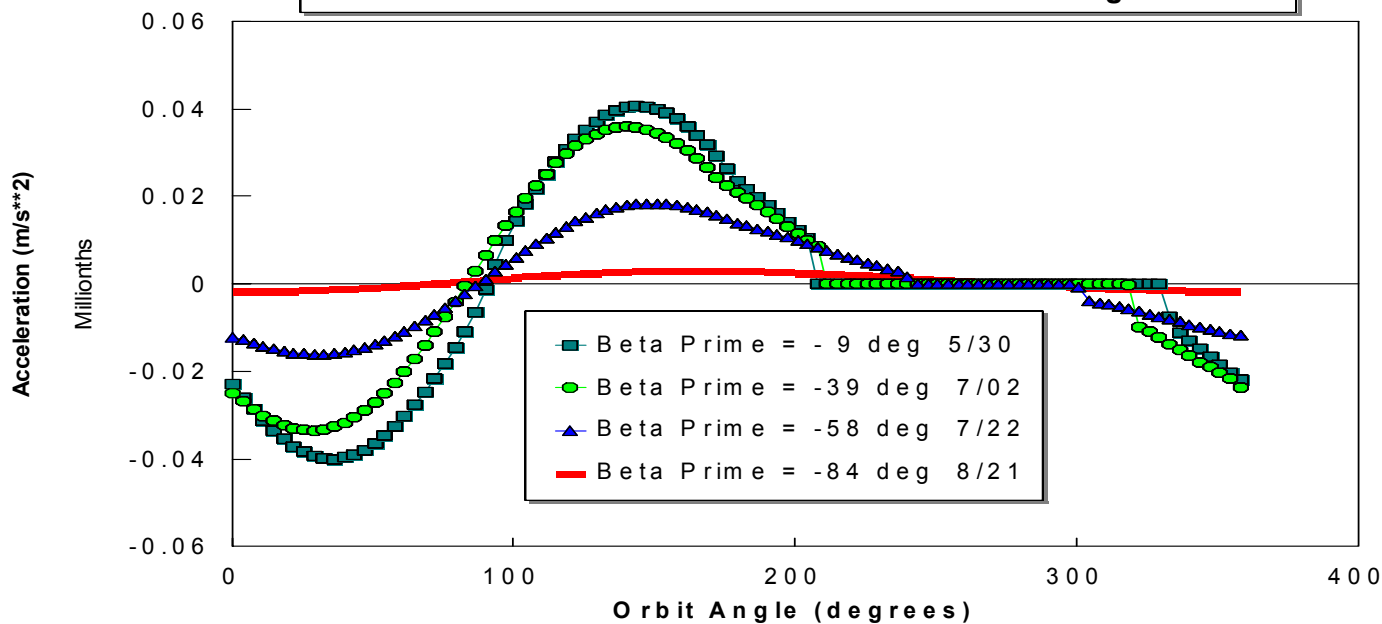


Figure 5. Laser Retroreflector Array Offset to Spacecraft Center of Mass Vector

LRA Offset Estimated using June '98 SLR Data

Description	Spacecraft Body-fixed Coordinates (cm)			SLR residual	SLR residual
	X	Y	Z	Mean (cm)	RMS (cm)
A priori CoM	89.7	0.8	-6.6		
A priori offset	114.2	77.2	42.7	-2.5	10.7
Estimated offset	107.9	76.1	53.3	-0.1	10.0

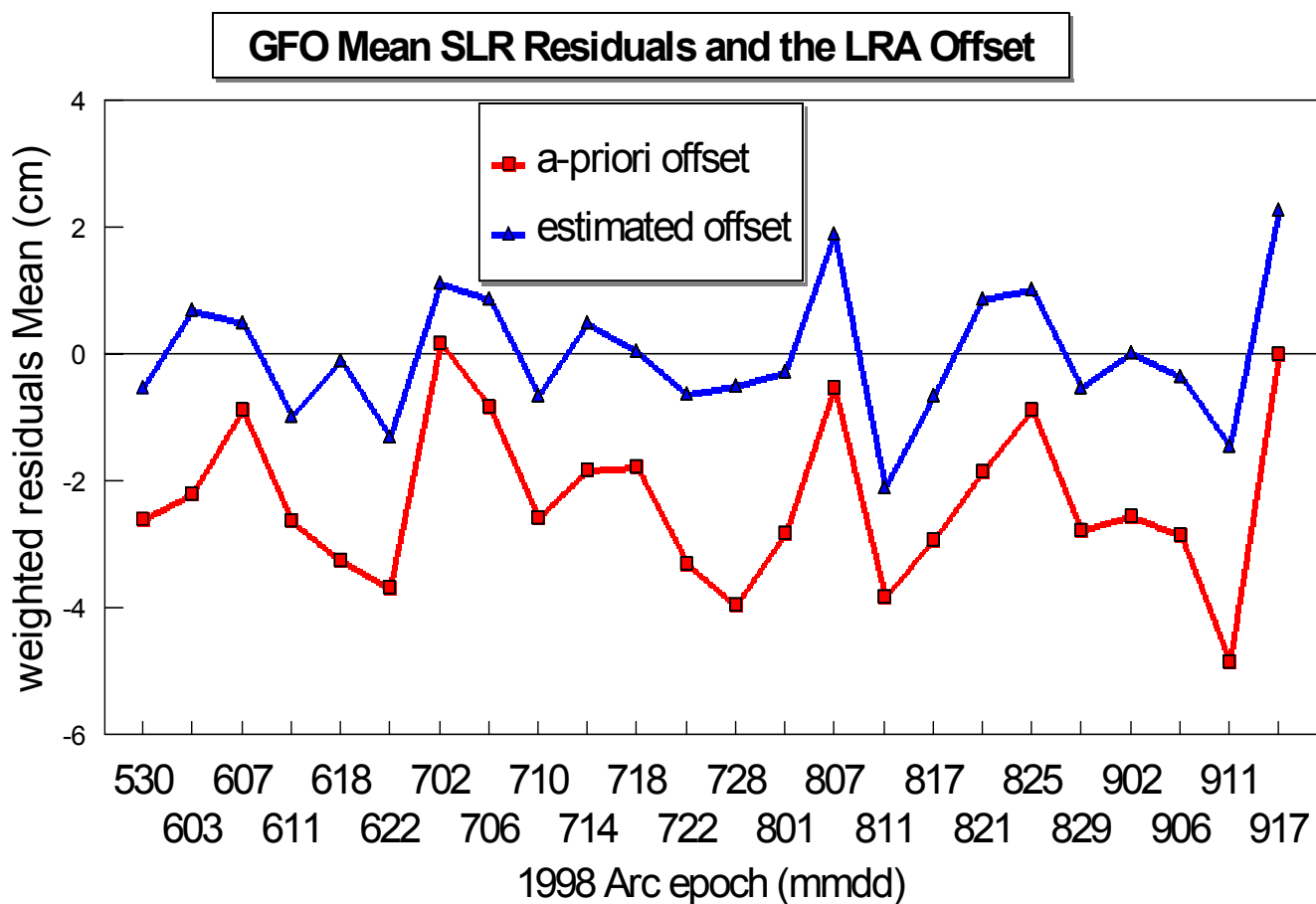
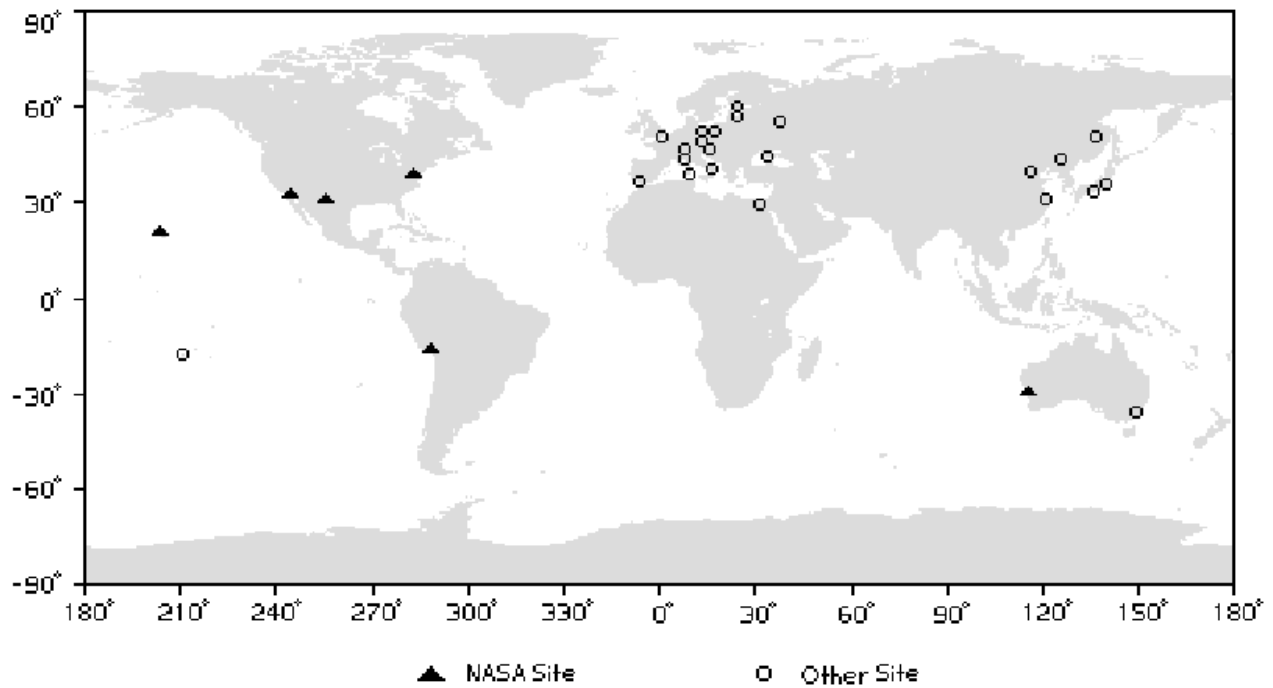


Figure 6. SLR Network Tracking GFO



GFO SLR Tracking History

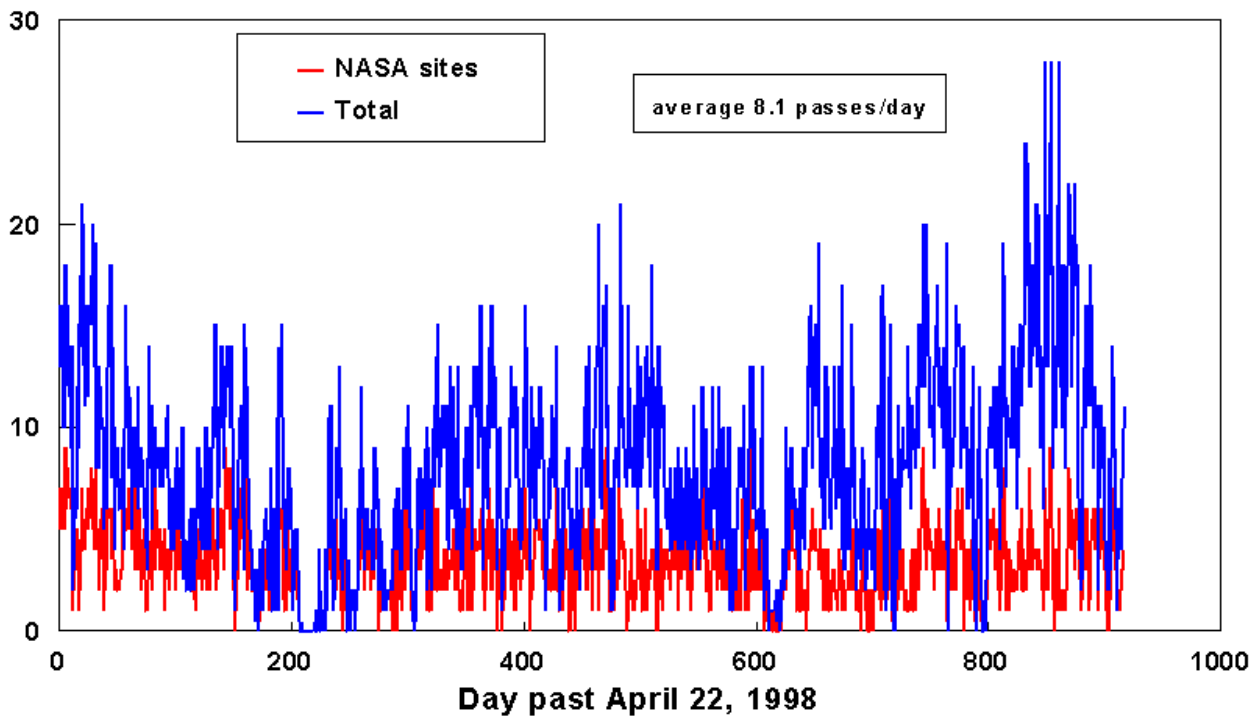


Figure 7. GFO SLR Passes by Station

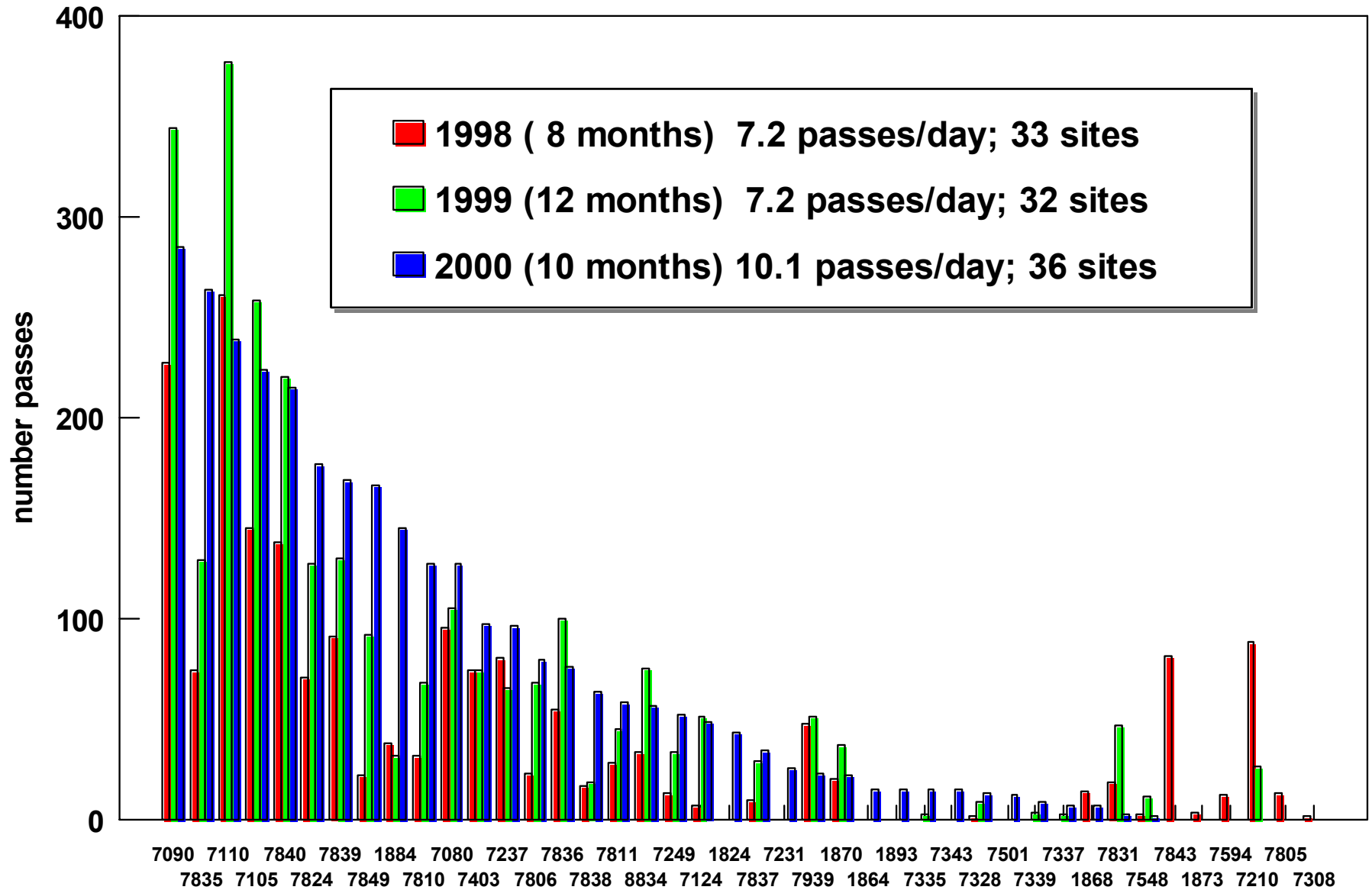
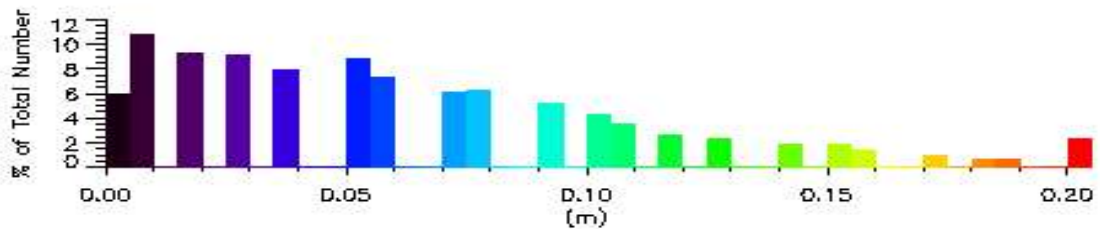
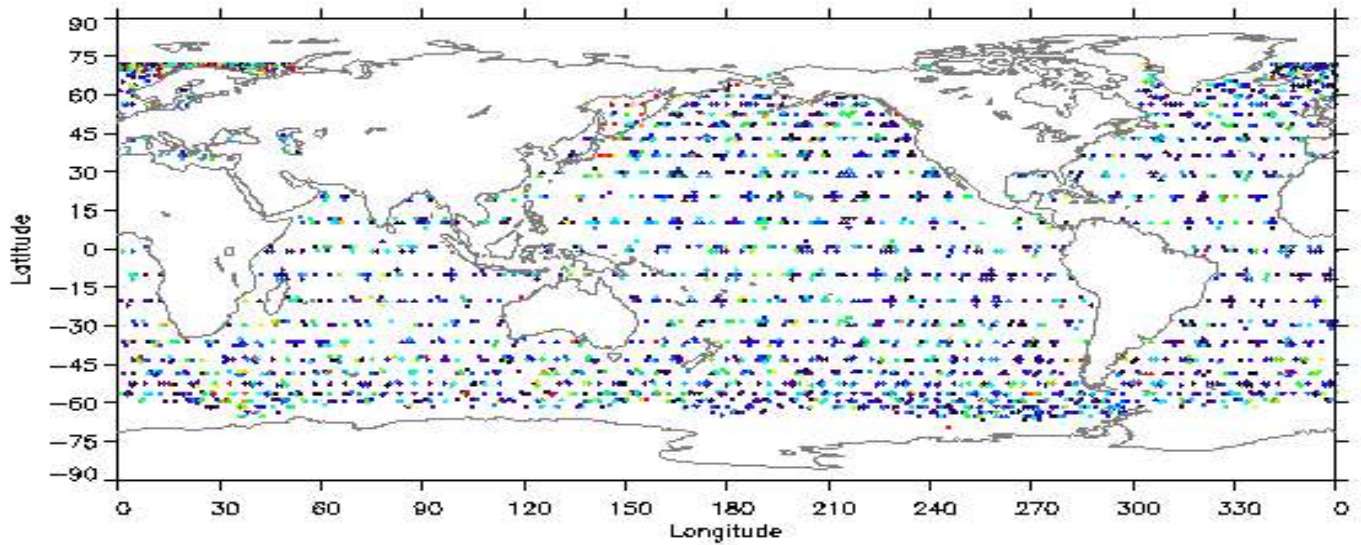


Figure 8. GFO Altimeter Crossover [Residuals]



RMS: 0.082 (m) Number Points: 3060 Span: 990616-990703

TP+ERS Sea Surface Height Variability

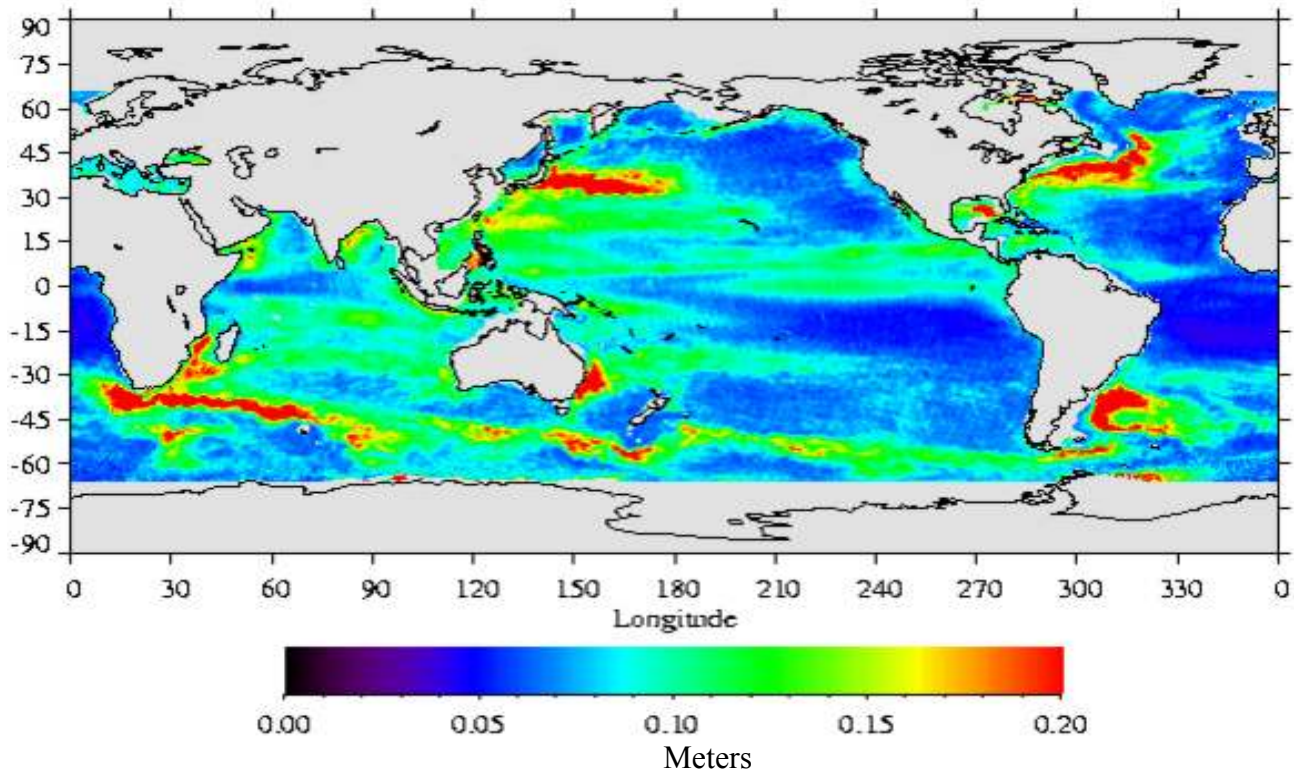


Figure 9. Gravity error does not explain variation in fits

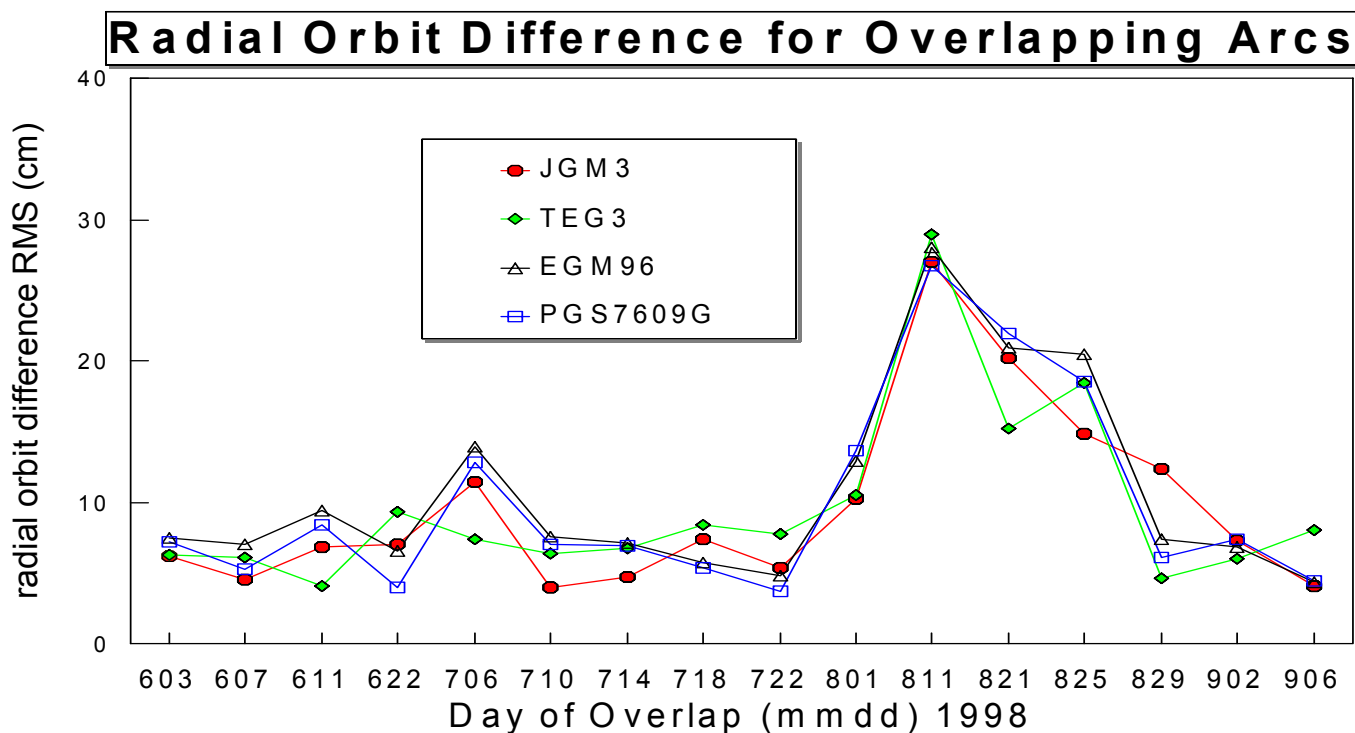
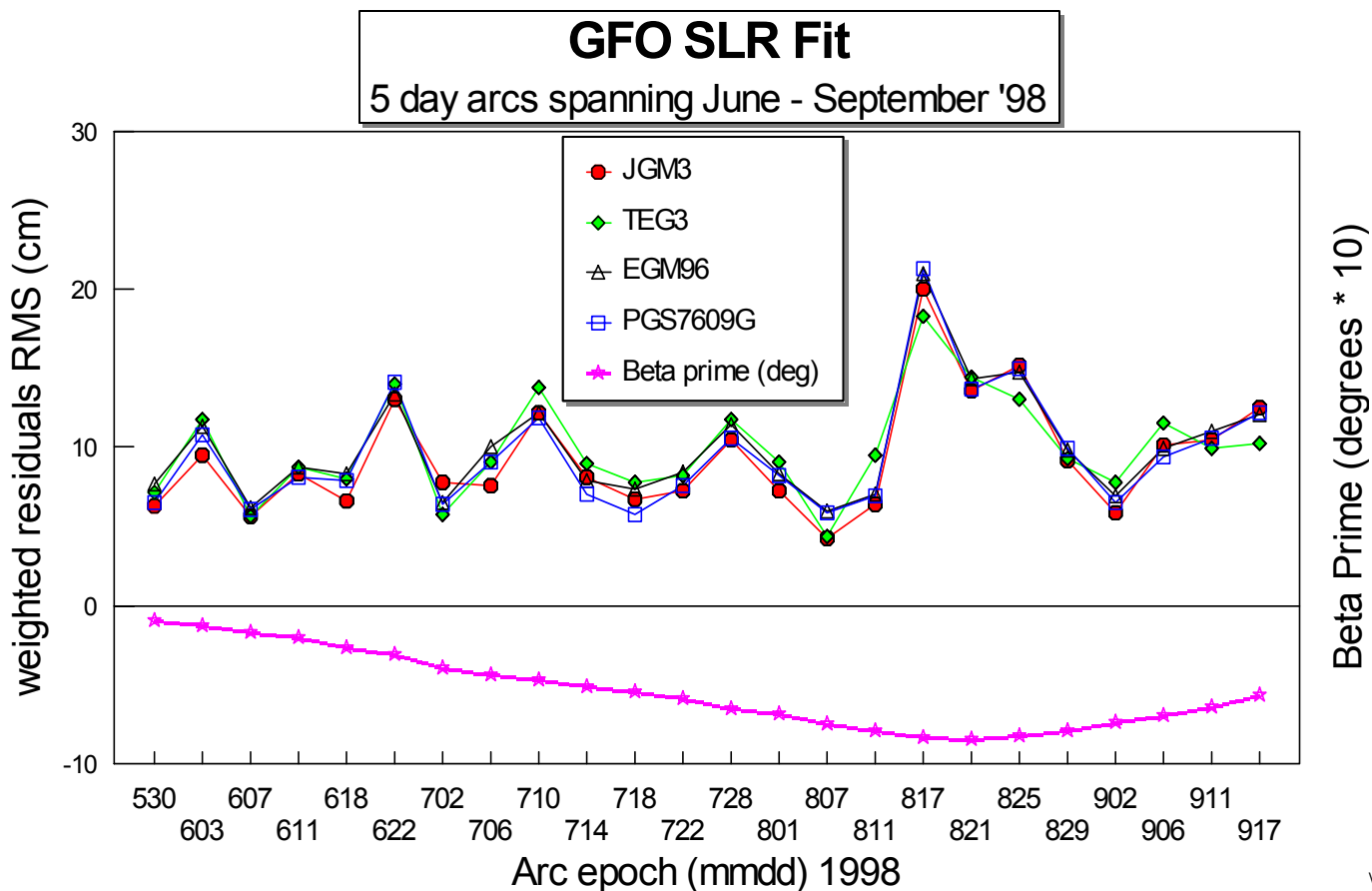
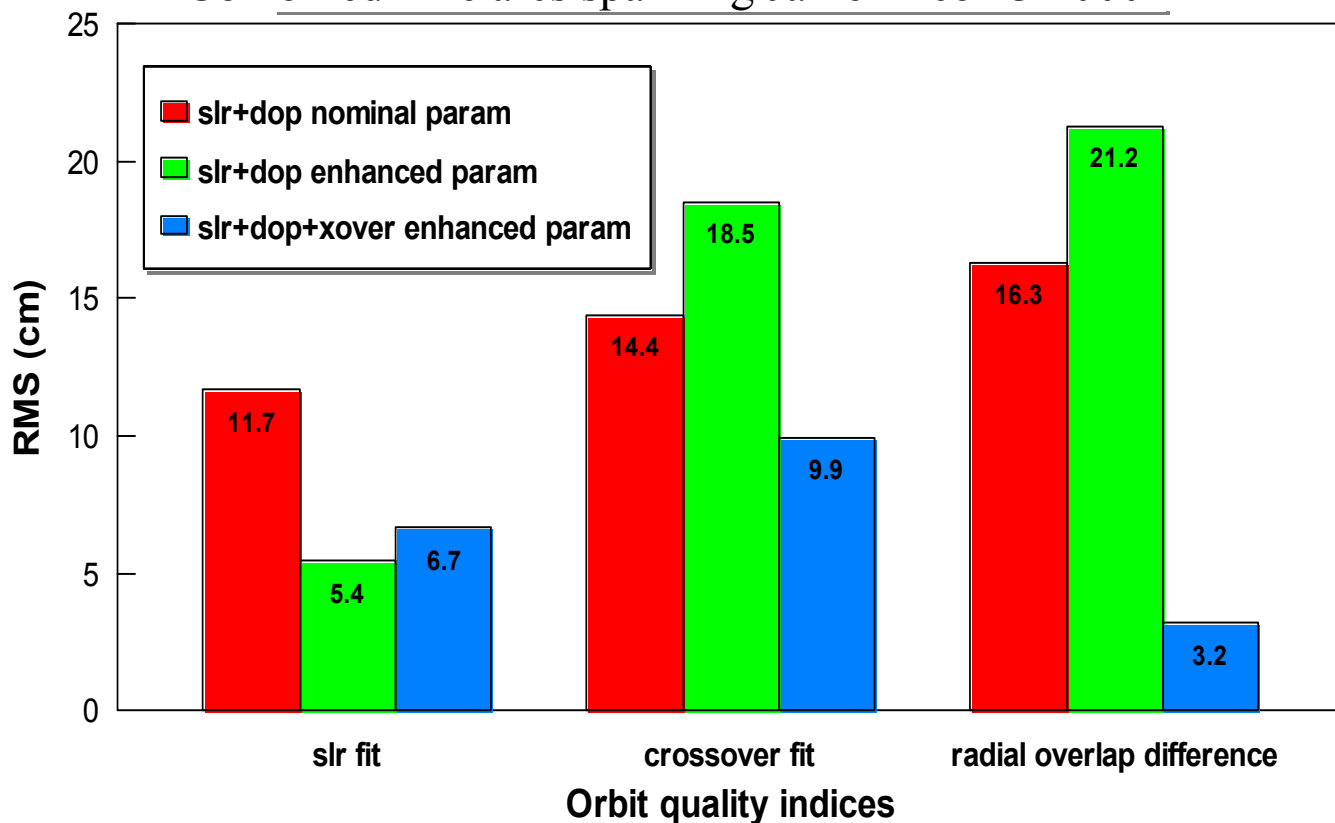


Figure 10. GFO Orbit Solution Strategies

nominal: 1drag/day, 1cpr/5day; enhanced: 3drag/day, 1cpr/1day

Combined nine arcs spanning Jan 6 –Feb 13 2000



Combined 2 arcs spanning May 5 –May 17, 2000

Data combination & POD strategy	Doppler fit (cm/s)	SLR fit (cm)	X-over fit (cm)	Orbit RMS difference w.r.t. dop+slr+xover orbit (cm)		
				radial	cross-track	along-track
doppler+slr+xover <i>adjust</i> 3 drag/day, 1 cpr/day	1.72	5.08	9.86	----	----	----
doppler+slr <i>adjust</i> 2 drag/day, 1 cpr/arc	1.72	9.56	12.42	4.6	8.5	42.1
doppler+xover <i>adjust</i> 2 drag/day, 1 cpr/arc	1.72	39.02	10.3	12.1	62.1	79.8
doppler <i>adjust</i> 1 drag/day, 1 cpr/arc	1.72	47.62	54.57	30.9	54.4	115.7

Figure 11. Orbit accuracy limited by sparse SLR tracking
GFO-GFO Altimeter Crossover Differences

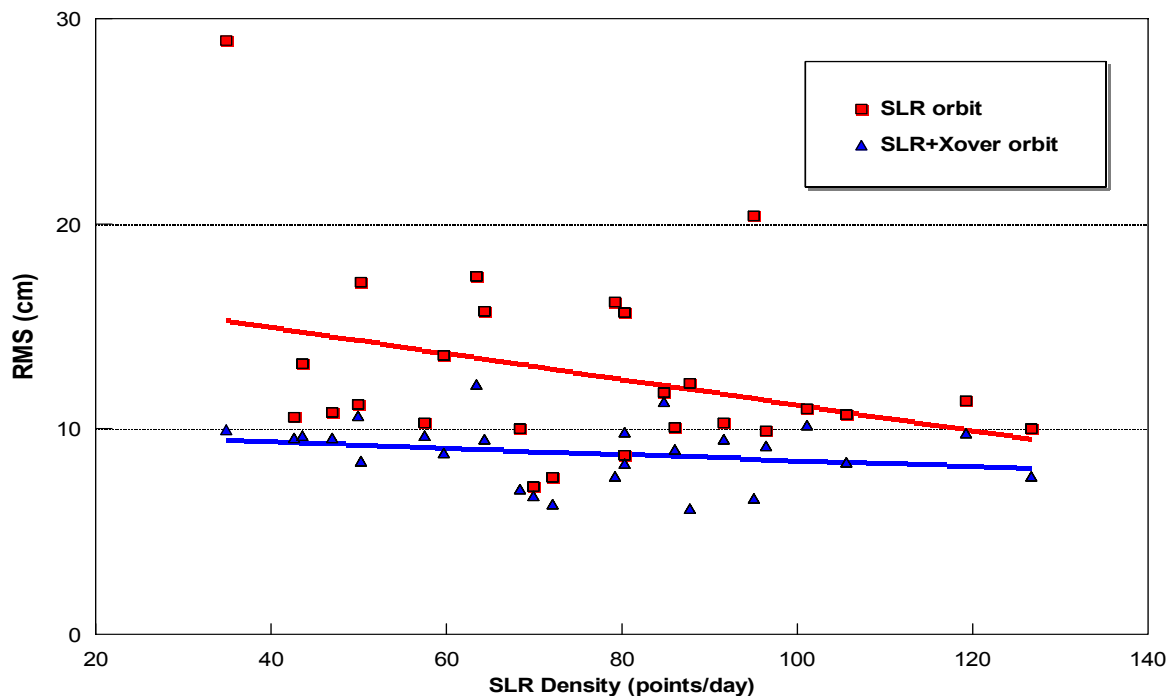


Figure 12. GFO macro-model parameter sensitivity
Uncorrelated Weighted Variance

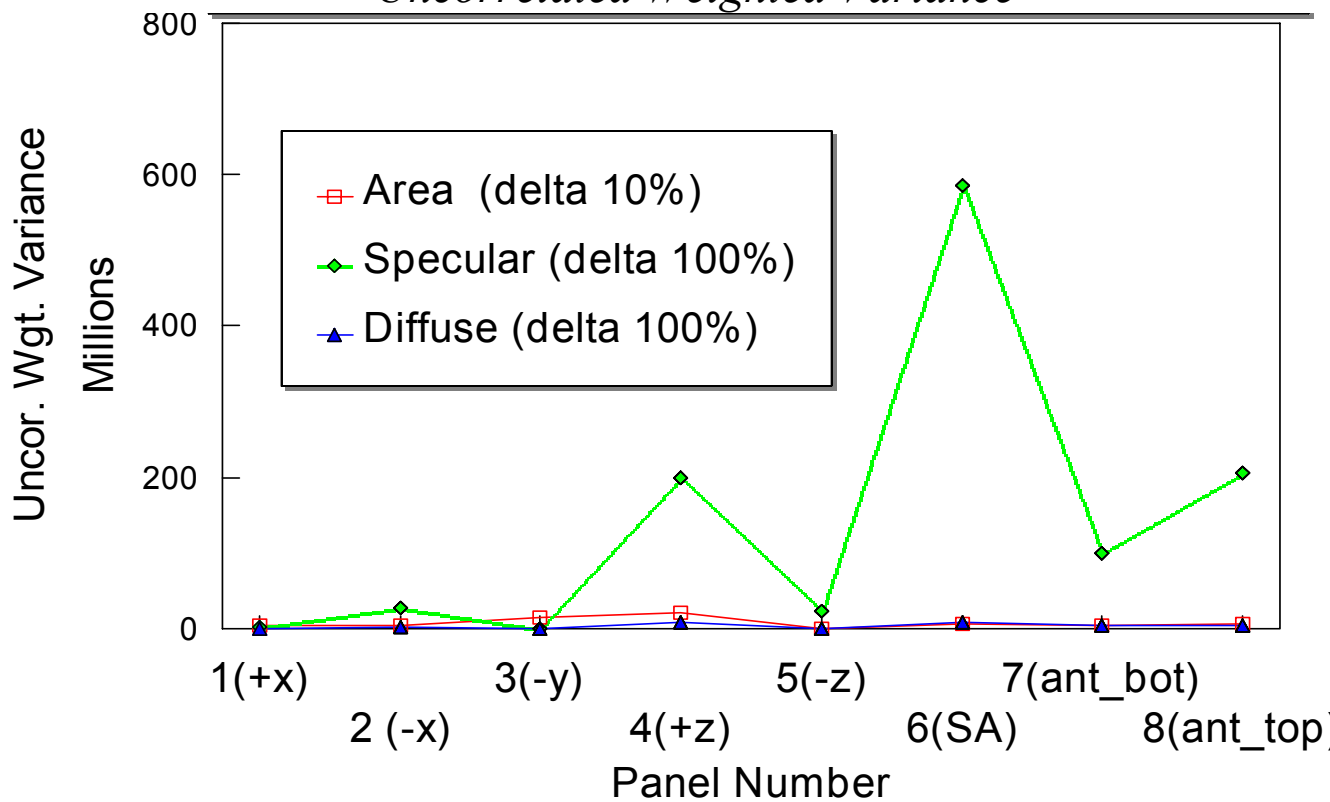


Figure 13. GFO Macro model Tuning

spacecraft surface model	solar array (SA) reflectivity coefficient	SLR fits over 23 dependant arcs (cm)	SLR fits over 57 independent arcs (cm)	SLR fits over 80 arcs total ² (cm)
cannonball	----	13.23	12.88	12.99
a-priori macro model	.160	13.11	12.89	12.95
tuned SA macro model ₁	.144	13.04	12.80	12.87

- 1) tuned using 23 SLR+Doppler and 8 SLR+Doppler +Crossover arcs spanning 980522 – 000206
- 2) 80 consecutive arcs spanning 980422 – 990603

SLR Fit Improvement over Cannonball model

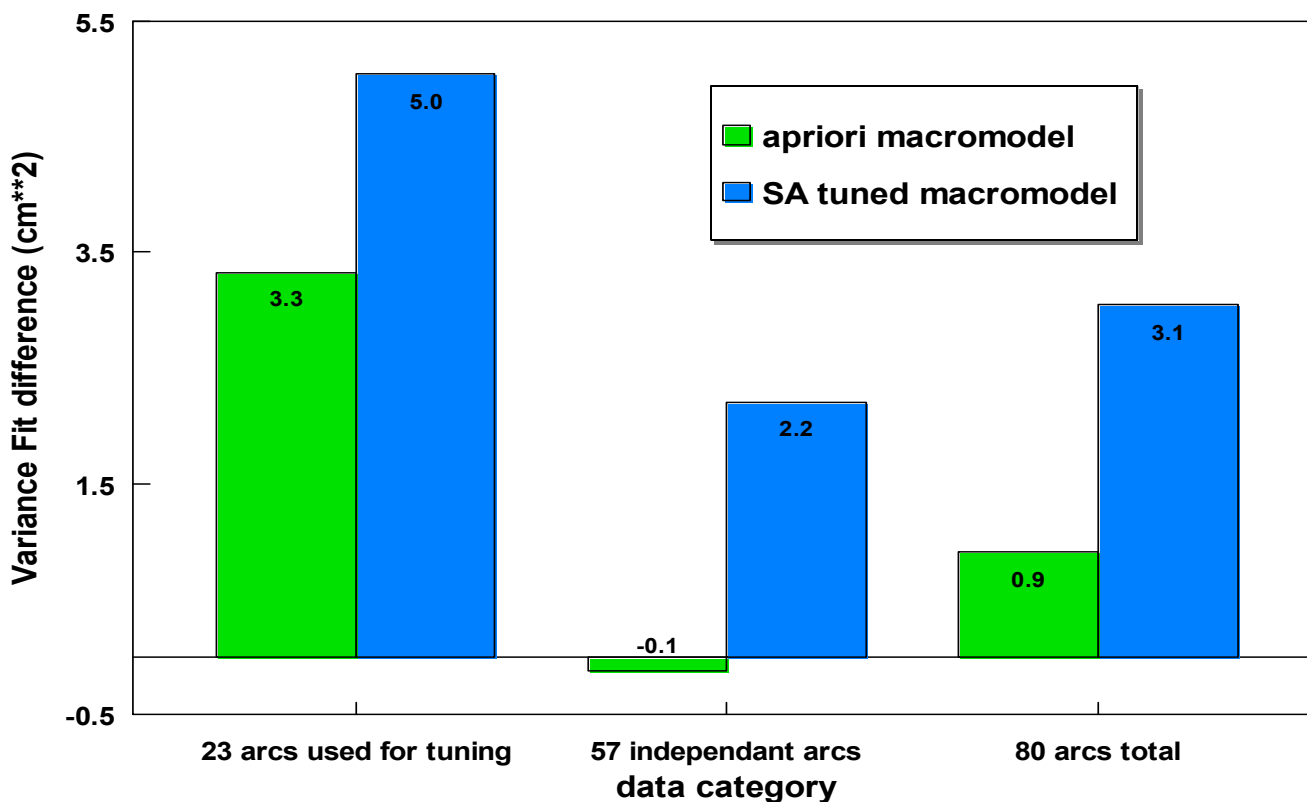


Figure 14. Recovered Empirical Accelerations vary with Beta'

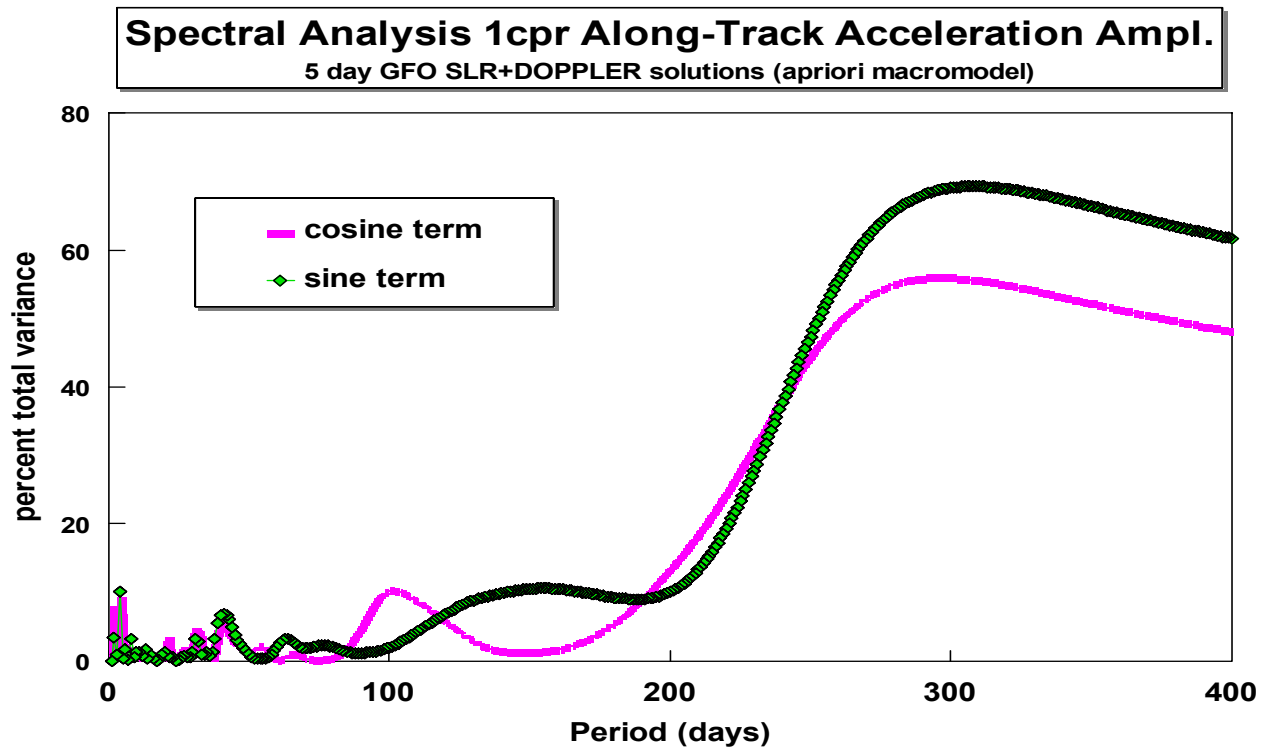
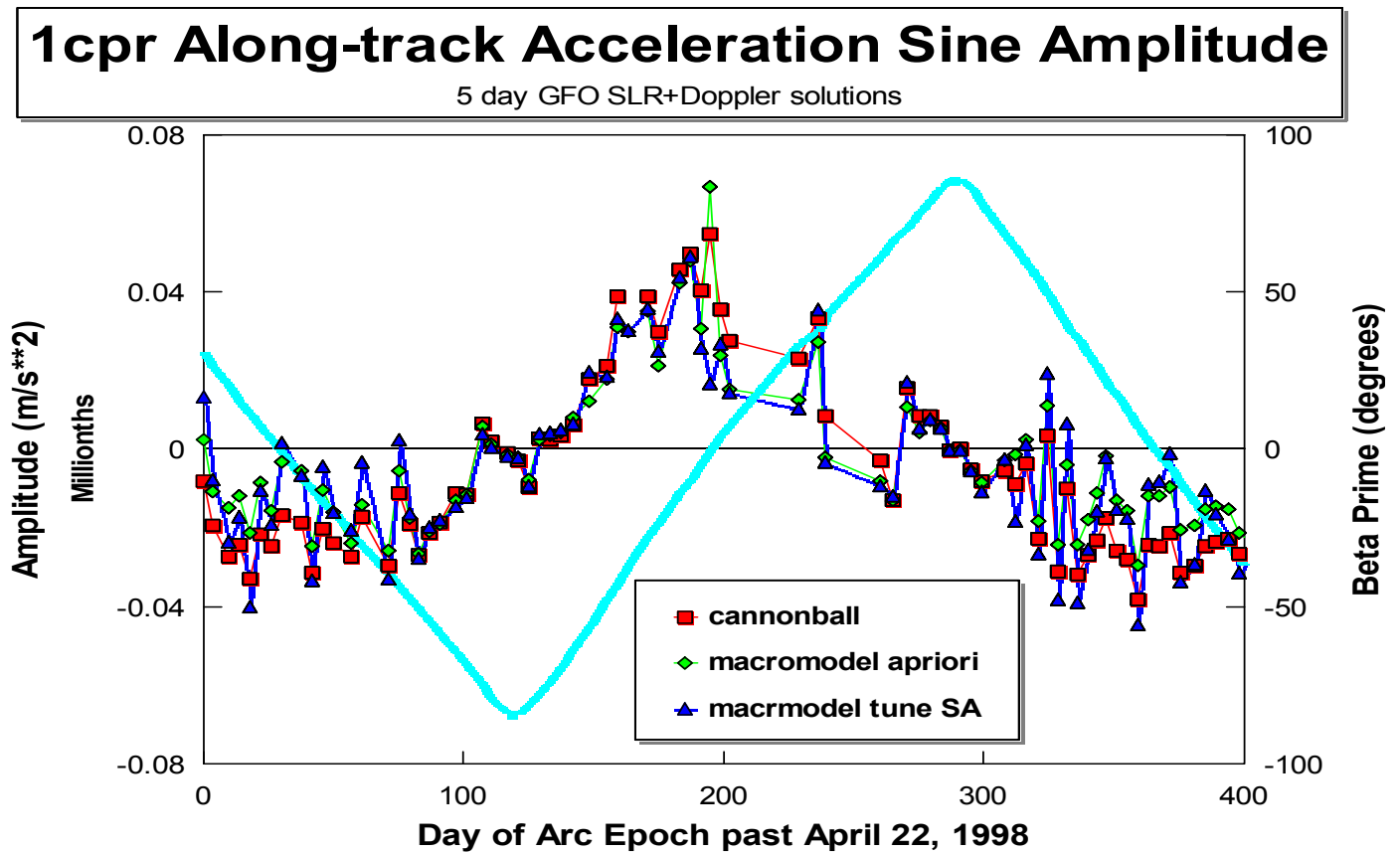


Figure 15. Empirical Acceleration Amplitude and Phase retain strong Beta' signal

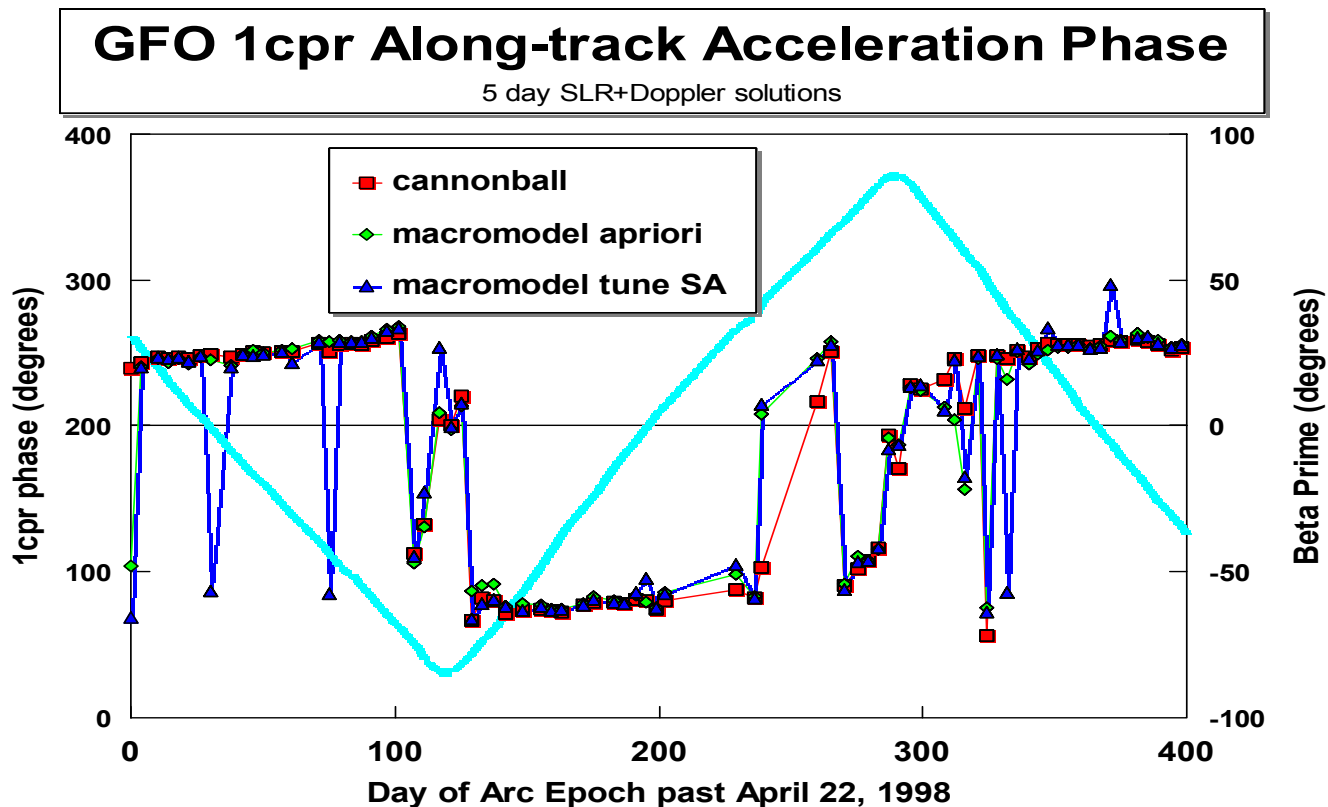
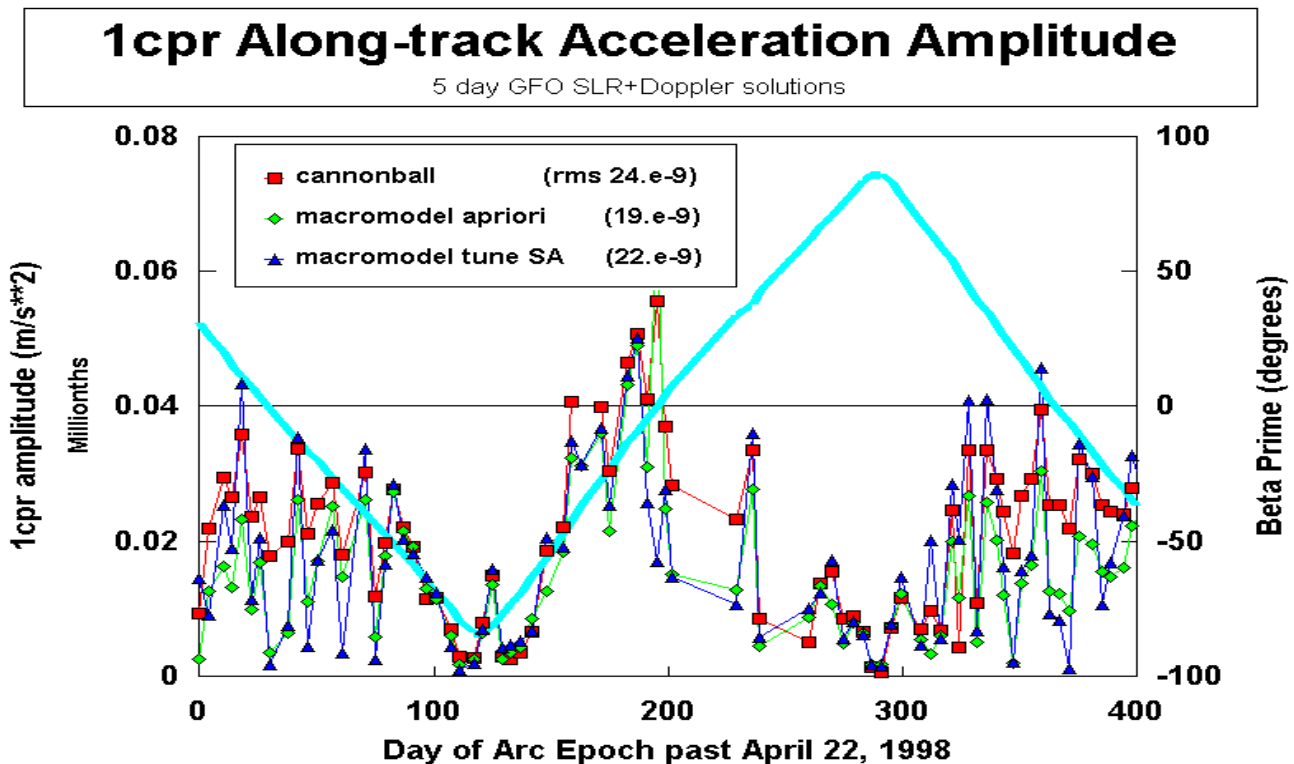
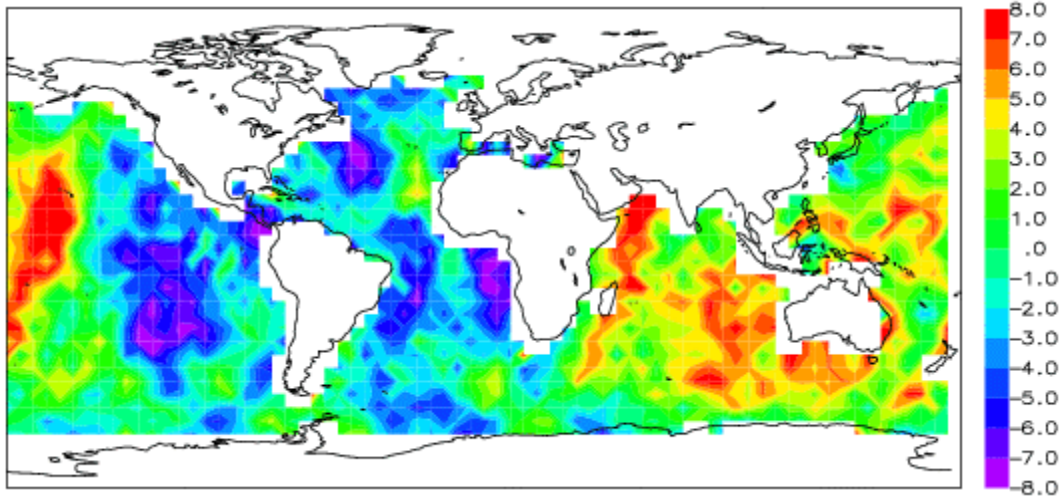
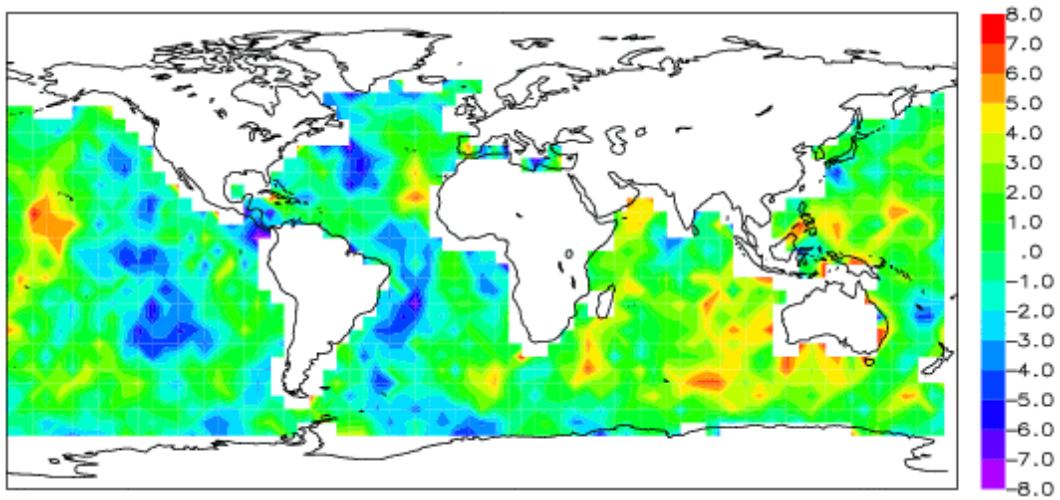


Figure 16. GFO geographically correlated orbit error

PGS7609G TOPEX-GFO altimeter crossover difference (cm)



PGS7723C TOPEX-GFO altimeter crossover difference (cm)



PGS7723C - PGS7609G radial orbit difference (cm)

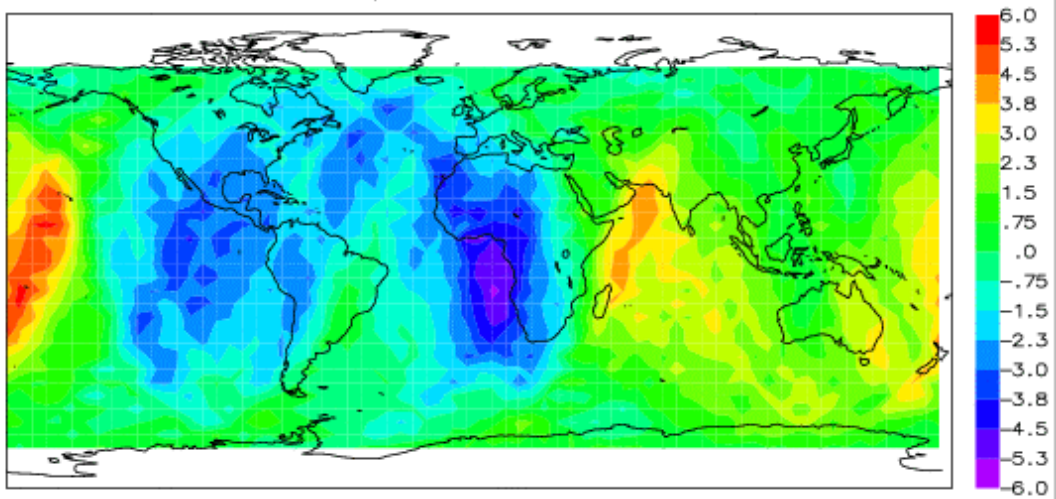
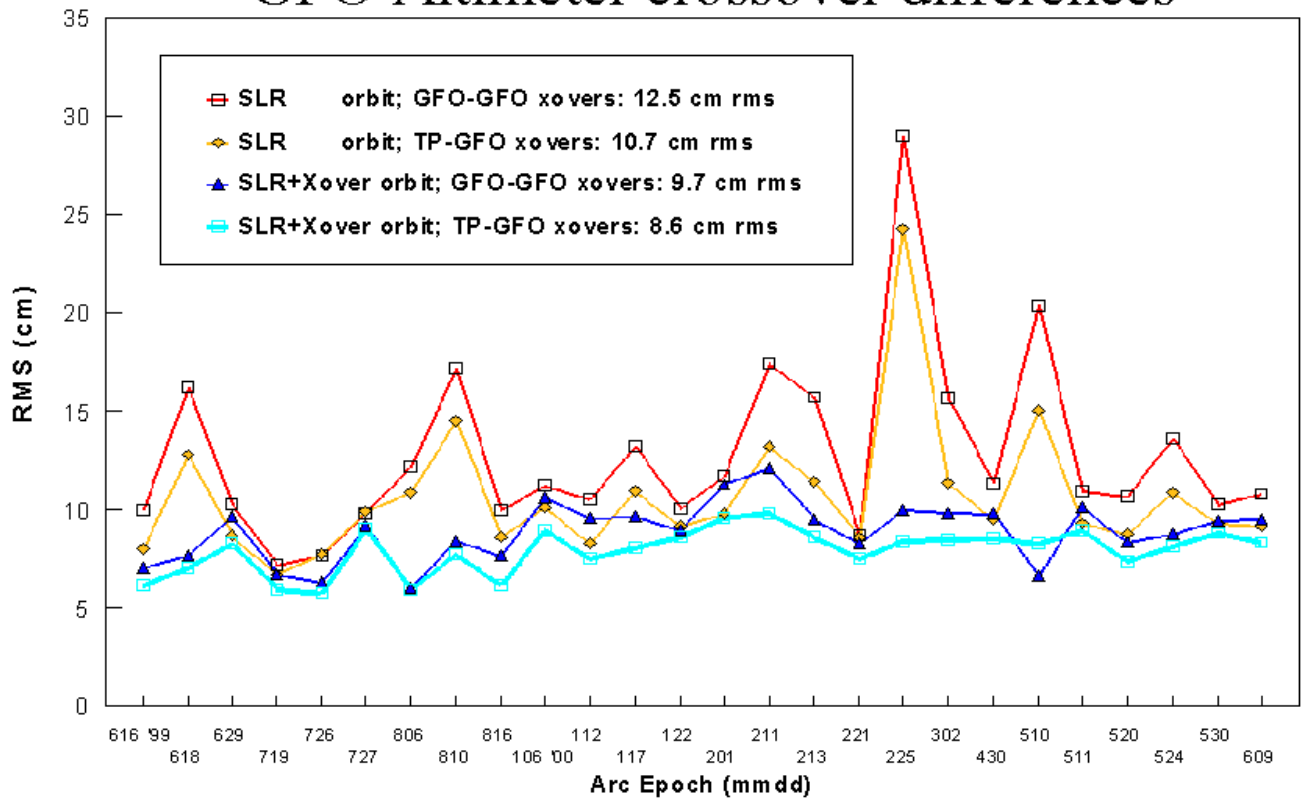
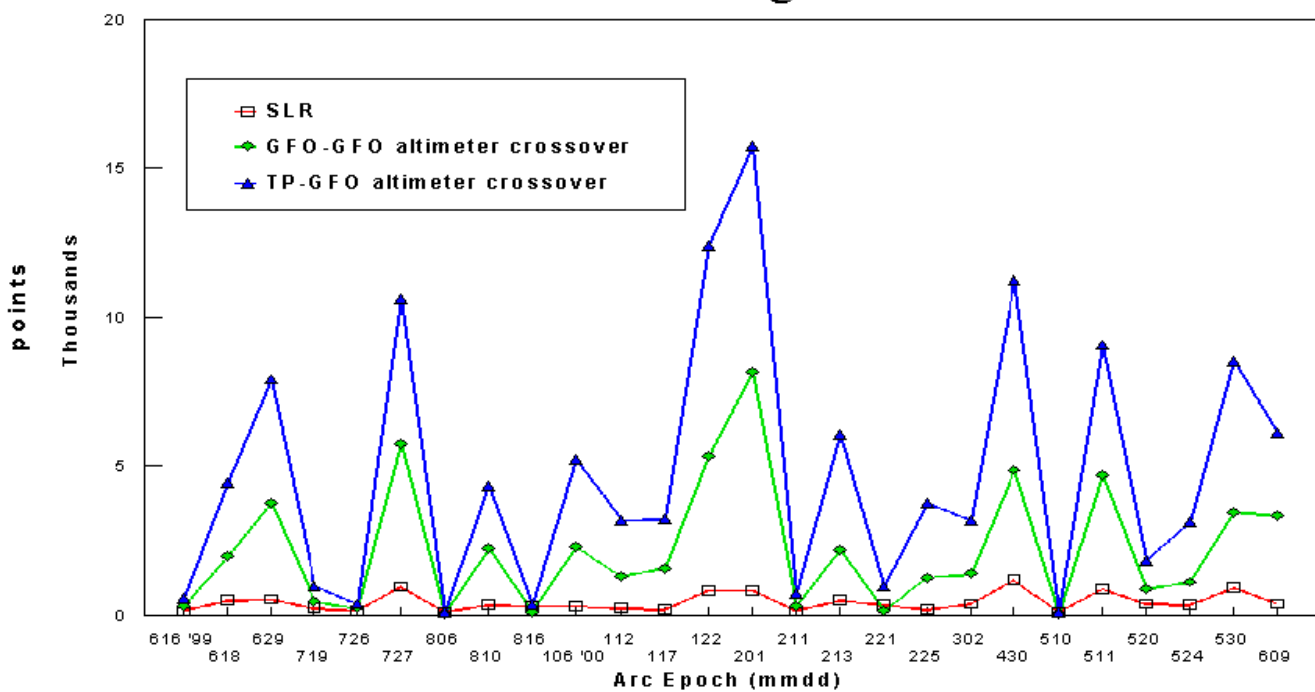


Figure 17. GFO crossover data significantly helps POD

GFO Altimeter crossover differences



GFO Tracking Data



REFERENCES

1. Frazier W., Mitchell S., Weiss M., Wiener D., "Initialization and Early On-Orbit Performance of the Geosat Follow-On Satellite", *22nd AAS Guidance and Control Conference*, Feb '99, Breckenridge, Colorado, AAS 99-072.
2. Zelensky N.P., Luthcke S.B., Gehrman L., Rowlands D.D., Marshall J.A., Lemoine F.G., "Error Analysis of the GEOSAT Follow-On Satellite Orbit Determined Using SLR and GPS Tracking (abstract)," *Annales Geophysicae EGS XXII General Assembly*, Vol 15, suppl. 1, pp. C187, April 1997.
3. D.E. Pavlis, S. Lou, P. Dahiroc, J.J. McCarthy, and S.B. Luthcke, GEODYN operation manuals, five volumes, Raytheon ITSS, December 18, 1998.
4. F.G. Lemoine, S.C. Kenyon, J.K. Factor, R.G. Trimmer, N.K. Pavlis, D.S. Chinn, C.M. Cox, S.M. Klosko, M.H. Torrence, Y.M. Wang, R.G. Williamson, E.C. Pavlis, R.H. Rapp, and T.R. Olson, *The Development of the Joint NASA GSFC and NIMA Geopotential Model EGM96*, NASA/TP-1998-206861, July, 1998, NASA Goddard space Flight Center, Greenbelt, MD.
5. B.D. Tapley, C.K. Shum, J.C. Ries, S.R. Poole, P.A.M. Abusali, S.V. Bettadpur, R.J. Eanes, M.C. Kim, H.J. Rim, and B.E. Schutz, "The TEG-3 geopotential model," in *Gravity, Geoid, and Marine Geodesy* J. Segawa, H. Fujimoto, and S. Okubo (eds.), Vol 117, *International Association of Geodesy Symposia*, Springer-Verlag, Berlin, 453-460, 1997.
6. B.D. Tapley, M.M. Watkins, J.C. Ries, G.W. Davis, R.J. Eanes, R. Poole, H.J. Rim, B.E. Schutz, C.K. Shum, R.S. Nerem, F.J. Lerch, J.A. Marshall, S.M. Klosko, N.K. Pavlis, and R.G. Williamson, The Joint Gravity Model-3, *J. Geophys Res.*, 101(B12), 28029-28049, 1996.
7. J.A. Marshall and S.B. Luthcke "Modeling Radiation Forces Acting on TOPEX/POSEIDON for Precision Orbit Determination," *Journal of Spacecraft and Rockets*, Vol 31, No. 1, 1994, pp. 99-105.
8. J.A. Marshall and S.B. Luthcke "Radiative Force Model Performance for TOPEX/POSEIDON for Precision Orbit Determination," *Journal of Astronomical Sciences*, Vol. 42, No. 2, 1994, pp. 229-246.
9. J.A. Marshall, N.P. Zelensky, S.M. Klosko, D.S. Chinn, S.B. Luthcke, K.E. Rachlin, R.G. Williamson, "The temporal and spatial characteristics of TOPEX/POSEIDON radial orbit error," *JGR*, Vol. 100, No. C12, pp. 25331-25252, Dec. 1995.
10. F.G. Lemoine, N.P. Zelensky, D.D. Rowlands, G.C. Marr, S.B. Luthcke, C.M. Cox, "Precise Orbit Determination for the GEOSAT Follow-On Spacecraft", 1999 Flight Mechanics Symposium Proceedings, NASA GSFC NASA/CP-1999-209235, pp. 495-507, May 1999
11. NASA SLR Satellite Information web page, http://ilrs.gsfc.nasa.gov/slr_sats/slr_satellites.html
12. Colombo, O.L., "Ephemeris errors of GPS satellites," *Bull. Geod.*, 60, 64-84, 1986.
13. S.B. Luthcke, J.A. Marshall, S.C. Rowton, K.E. Rachlin, C.M. Cox, R.G. Williamson, "Enhanced Radiative Force Modeling of the Tracking and Data Relay satellites", *JAS* Vol. 45, No. 3, July-September 1997, pp. 349-370
14. Ray, R.D., "A Global Ocean Tide Model from TOPEX/POSEIDON Altimetry: GOT99.2," NASA/TM-1999-209478, NASA/GSFC Sep 1999.
15. Hedin, A.E., "The atmosphere model in the region 90 to 200 km," *Adv. Space Res.*, 8(5), 9-25, 1988